LEVEL III
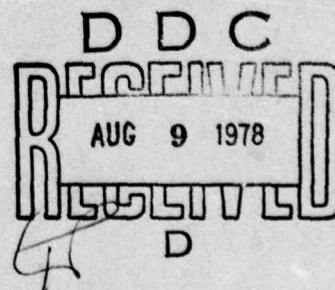
RADC-TR-77-420
Final Technical Report
December 1977

PO26748

MICROWAVE ACOUSTIC AND BULK DEVICE
TECHNIQUE STUDIES

Edward L. Ginzton Laboratory

Approved for public release; distribution unlimited.

D D C
RECEIVED
AUG 9 1978
D

ROME AIR DEVELOPMENT CENTER
AIR FORCE SYSTEMS COMMAND
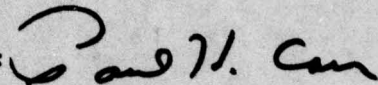GRIFFISS AIR FORCE BASE, NEW YORK 13441

78 08 03 18

This report has been reviewed by the RADC Information Office (OI) and is releasable to the National Information Service (NTIS). At NTIS it will be releasable to the general public, including foreign nations.
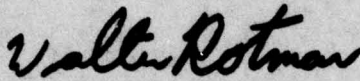
This technical report has been reviewed and approved for publication.
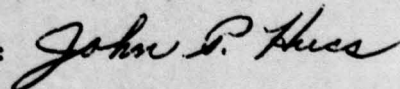
APPROVED: *[signature]*
PAUL H. CARR
Contract Monitor
Antennas and RF Components Branch
Electromagnetic Sciences Division

APPROVED: *[signature]*
WALTER ROTMAN, Chief
Antennas and RF Components Branch
Electromagnetic Sciences Division

FOR THE COMMANDER: *[signature]*
JOHN P. HUSS
Acting Chief, Plans Office

REPORT DOCUMENTATION PAGE	READ INSTRUCTIONS BEFORE COMPLETING FORM

1. REPORT NUMBER	2. GOVT ACCESSION NO.	3. RECIPIENT'S CATALOG NUMBER
RADC-TR-77-420		

4. TITLE (and Subtitle)	5. TYPE OF REPORT & PERIOD COVERED
MICROWAVE ACOUSTIC AND BULK DEVICE TECHNIQUE STUDIES,	FINAL REPORT, - 1 Nov. 1973 - 30 Sep 1977,
	6. PERFORMING ORG. REPORT NUMBER
	G. L. 2748

7. AUTHOR(s)	8. CONTRACT OR GRANT NUMBER(s)
Multiple Authors	F30602-74-C-0038

9. PERFORMING ORGANIZATION NAME AND ADDRESS	10. PROGRAM ELEMENT, PROJECT, TASK AREA & WORK UNIT NUMBERS
Stanford University Edward L. Ginzton Laboratory Stanford, California 94305	62702F 55730707

11. CONTROLLING OFFICE NAME AND ADDRESS	12. REPORT DATE
Deputy for Electronic Technology (RADC) Hanscom AFB, Massachusetts 01731 Monitor/Paul Carr/EEA	December 1977
	13. NUMBER OF PAGES

14. MONITORING AGENCY NAME & ADDRESS(if different from Controlling Office)	15. SECURITY CLASS. (of this report)
	UNCLASSIFIED
GL-2748 63 p.	15a. DECLASSIFICATION/DOWNGRADING SCHEDULE N/A

16. DISTRIBUTION STATEMENT (of this Report)

Approved for public release; distribution unlimited.

17. DISTRIBUTION STATEMENT (of the abstract entered in Block 20, if different from Report)

Marvin/Chodorow H.J./Shaw

18. SUPPLEMENTARY NOTES

RADC Project Engineer: Paul H. Carr (ETEM)

19. KEY WORDS (Continue on reverse side if necessary and identify by block number)

Acoustic Amplifier	Analog-to-Digital	Interdigital Transducers
Acoustic Delay Lines	Conversion	Piezoelectric Films
Acoustic Parametric	Convolution	Pulse Compression
Interactions	Cross-correlation	Semiconductor Films
Acoustic Waves	Epitaxial Films	Signal Processing

20. ABSTRACT (Continue on reverse side if necessary and identify by block number)

The final report describes device research in both linear and nonlinear acoustic devices for signal processing. Wideband, monolithic surface-acoustic-wave convolvers have been developed, based on nonlinear interaction between surface acoustic waves and conduction electrons in zinc oxide film on sapphire structures achieving new ranges of conversion efficiency. A high speed 8-bit analog-to-digital converter has been developed, using a heretofore unused property of linear surface acoustic wave delay lines, which has potential for multichannel parallel processing with large data throughput.

DD FORM 1473   EDITION OF 1 NOV 65 IS OBSOLETE
1 JAN 73

EVALUATION

1. This report is the Final Report on the contract. It covers research done on acoustic surface wave devices during the period 1 Nov 73 to 30 Sep 77. The objective of the research is the generation of new device concepts and the analytical and experimental verification as to their ultimate usefulness for signal processing applications. Improvements were made in acoustic surface wave convolver efficiency. The surface wave convolver can be used for performing convolution/correlation, time reversal and Fourier analysis of arbitrary signals. A new approach which may lead to low cost, simplified analog/digital conversion has been devised. This combines a surface acoustic wave ramp generator and a digital counter. An 8-bit A/D conversion was performed in 2 usec.

2. The above work is of value since it provides basic knowledge which makes possible new and improved devices for signal processing. This increases the survivability of USAF surveillance and communications systems in a hostile electromagnetic environment.

PAUL H. CARR
Project Engineer

iii

TABLE OF CONTENTS

FOREWORD

This is the Final Report for Contract F30602-74-C-0038, Job Order Number 55730707, prepared by the Edward L. Ginzton Laboratory at Stanford University, Stanford, California, for Rome Air Development Center, Griffiss Air Force Base, New York. This report, whose secondary number is G. L. 2748, covers the period 1 November 1973 - 30 September 1977.

Professor Marvin Chodorow and Dr. H. J. Shaw are the co-responsible investigators for this contract. Paul H. Carr, ETEM, is the RADC Project Engineer.

I. INTRODUCTION

This contract has been concerned with research on devices utilizing both linear and nonlinear properties of surface acoustic waves. The nonlinear work was concerned mostly with the development of SAW convolvers, in monolithic form, utilizing the nonlinear properties of bulk semiconductors, and having higher efficiency and bandwidth than previously available. The linear work was concerned mainly with the development of analog-to-digital (A/D) converters involving a new application of surface acoustic waves which offers high speed conversion.

The nonlinear projects have been covered in previous reports under that contract, and will be only briefly summarized here together with reference to the reports and publications where further details may be found. The analog-to-digital conversion project, which remained active during the last semi-annual period under the contract, is covered in more detail herein.

- 1 -

II. MONOLITHIC SURFACE ACOUSTIC WAVE CONVOLVERS

A. INTRODUCTION

The surface acoustic wave convolver is a device which allows one to perform the cross-convolution of two arbitrary signals. This is an analog operation, carried out at high speed. In a typical application, one of the two signals can be a locally generated reference signal, and the other can be an unknown signal. Cross-convolution between the unknown signal and the reference signal is equivalent to the cross-convolution between the unknown signal and the time-reveresed version of the reference signal. Since the reference signal can be chosen at will electronically, the convolver introduces electronic agility into a number of operations which ordinarily impose fixed parameters locked to hardware configurations. For example, it is possible to carry out chirp pulse compression of arbitrary signals, in which the chirp rate and chirp profile can be changed electronically, from pulse to pulse if desired. SAW convolvers operate at high frequency and can have large bandwidth, so that real time operation is provided.

The acoustic convolver was originated[1] under an RADC research contract[2] which was a predecessor to the present Contract F30602-74-C-0038. This first work was done with bulk acoustic waves, and was extended to operation at frequencies in the GHz range.[3]

Surface acoustic wave convolvers can be constructed using either bulk acoustic waves or surface acoustic waves (SAW), the latter having advantages for operation in the UHF and VHF ranges. A SAW convolver consists basically of a two-port SAW delay line with an integrating electrode structure affixed in the space between the input and output transducers, and with means for optimizing the nonlinear interaction between surface acoustic waves propagating in the region covered by the integrating electrode.[4] An example is shown schematically in Fig. 1. The reference rf signal is introduced at one interdigital (ID) transducer, the unknown signal is introduced at the other transducer, and the cross-convolution is extracted from the center electrode.

B. BASIC MONOLITHIC CONVOLVER

Under the present contract, a new form of SAW convolver, using a zinc-oxide on silicon (ZnO/Si) structure, was developed. Prior to this, most SAW convolvers used a so-called separated medium structure. This consisted typically of a piezoelectric delay line over which a slice of silicon was placed,

---

[1]C. F. Quate and R. B. Thompson, Appl. Phys. Letters 16, 12, 494-496 (15 June 1970).

[2]Contract F30602-71-C-0125.

[3]J. M. White, D. K. Winslow, and H. J. Shaw, Proc. IEEE 60, 9, 1102-1103 (September 1972).

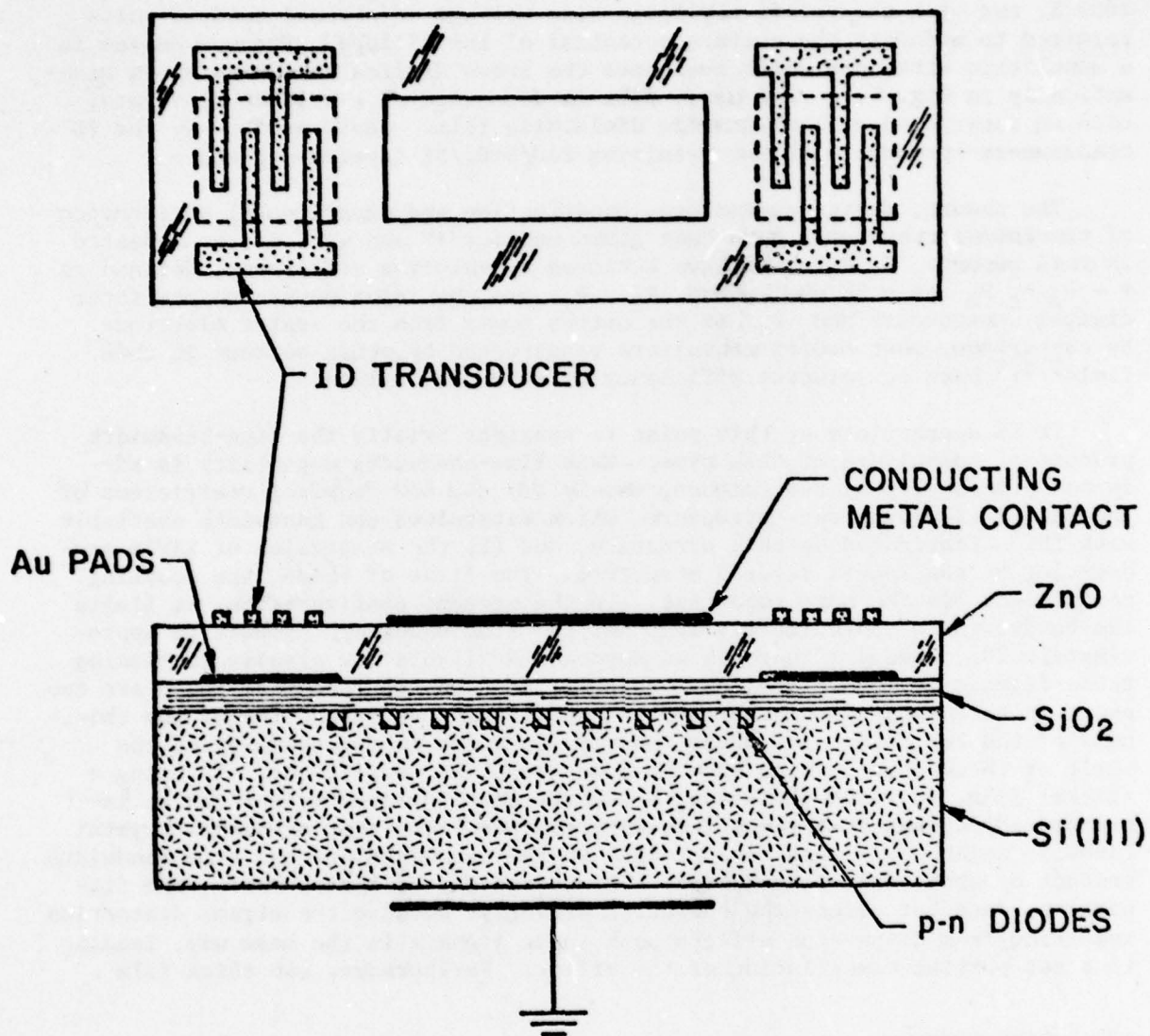[4]Gordon S. Kino and John Shaw, Scientific American 227, 4, 50-68 (Oct. 1972).

FIG. 1--Schematic of basic monolithic zinc oxide on silicon convolver.

uniformly spaced from the delay line by a small airgap. The purpose of the silicon is to provide a nonlinear interaction between SAW's on the delay line, as a result of coupling to the conduction electrons in the silicon. Such structures had problems with maintaining a uniform airgap of the order of 1000 $\overset{\circ}{A}$, and with the relatively large bias voltage of several hundred volts required to modulate the surface potential of the silicon. The new device is a monolithic structure which overcomes the above difficulties. As shown schematically in Fig. 1, a zinc oxide film is deposited on a silicon substrate, with an interposed silicon dioxide dielectric film. SAW's excited by the ID transducers propagate in the resulting $ZnO/SiO_2/Si$ layered structure.

The theory, design parameters, construction and experimental performance of the ZnO/Si convolvers have been given earlier[5,6] and will not be repeated in this report. Briefly, we have achieved convolution efficiency, defined as $F = P_3/P_1 P_2$ of $- 58$ dBm, where P_1, P_2 are the input powers to the inter-digital transducers and P_3 is the output power from the center electrode. By comparison, most ZnO/Si convolvers constructed by other workers in this field[7,8,9] have convolution efficiency of $- 70$ dBm or less.

It is appropriate at this point to consider briefly the time-bandwidth product of convolvers of this type. This time-bandwidth capability is affected principally by two factors, namely (1) the SAW coupling coefficient of the ZnO/Si film/substrate structure, which determines the bandwidth available with IDT's fabricated on this structure, and (2) the dispersion of SAW's propagating on the ZnO/Si layered structure. The first of these, the coupling coefficient, is the more important. In the present configuration, it limits the bandwidth to approximately 10%, and the time bandwidth product to approximately 20. However, there is an approach available for greatly increasing these figures in future devices. This is based on the fact that there are two peaks in the magnitude of the coupling coefficient as a function of the thickness of the ZnO film. The present device operates in the vicinity of the first of these peaks, which has the lower coupling coefficient. By using a thicker film, to reach the second peak, the coupling coefficient can be increased approximately 5 times (becoming comparable to that of single-crystal $LiNbO_3$), which would lead to increases in the bandwidth and the time bandwidth product by about this same factor. The second factor listed above, the dispersion, does not affect the operation strongly, because the signal distortion resulting from dispersion affects both input signals in the same way, leading to a net partial cancellation of the effect. Furthermore, the thick film

---

[5] Interim Technical Reports 1 through 5, Contract F30602-74-C-0038 (1 November 1973 - 30 April 1976).

[6] B. T. Khuri-Yakub and Gordon S. Kino, IEEE Trans. on Sonics and Ultrasonics SU-24, 1, p. 34 (January 1977).

[7] B. T. Khuri-Yakub and G. S. Kino, Appl. Phys. Letters 25, 188 (1974).

[8] L. A. Coldren, Appl. Phys. Letters 25, 473 (1974).

[9] K. L. Davis, Appl. Phys. Letters 26, 143 (1975).

approach would also result in a substantial reduction in the dispersion effect for each of the input signals.

C. WAVEGUIDE MONOLITHIC CONVOLVER

Experiments were carried out on a modified form of ZnO/Si convolver, in which the zinc oxide, originally deposited over the entire surface of the substrate, was etched to form a SAW waveguide.[10] This allows the SAW beam width w to be decreased in the interaction region, and theory indicates that this should increase the convolver efficiency in proportion to w^{-2}. The resulting device is illustrated in Fig. 2. The waveguide width is reduced by a factor of 10 below that of the SAW beam at the interdigital transducers, which should yield a 20 dB improvement in convolver efficiency over a normal convolver with a beam width equal to the transducer width, after accounting for the insertion loss of the ID transducers. Such an improvement was observed in the experimental devices.[11]

D. NEW METHOD FOR WIDEBAND EXCITATION OF INTERDIGITAL SURFACE ACOUSTIC WAVE TRANSDUCERS

It has been shown by Reeder, et al.,[12] that a wide bandwidth match to an acoustic transducer can be obtained by using a lumped element approximation of the transmission line inverter between the source and the transducer. In the approach developed in this work, the values of the lumped elements of the tuning network are chosen by using an optimization computer program. This program was originally developed at Hewlett Packard Co. for other purposes. Values of the components are optimized for minimum mismatch loss over the bandwidth of interest, after several iterations. The computation takes account of the fact that the acoustic radiation resistance varies with frequency. Thus, the filter network gives a lower mismatch loss on both sides of center frequency than at the center frequency where the transducer is more efficient. It is then possible to obtain an interdigital transducer bandwidth for N finger pairs larger than the f_0/N normally considered to be the optimum value.

Filter networks were designed and constructed for use with interdigital transducers on ZnO/Si and lithium niobate ($LiNbO_3$) media.[13] In the ZnO/Si case a bandwidth of 22 MHz was achieved at center frequency of 125 MHz, some three times better than obtained with simple inductance tuning. For $LiNbO_3$, the bandwidth was 39 MHz at center frequency of 100 MHz.

---

[10] Interim Technical Report No. 4, Contract F30602-74-C-0038 (1 May 1975 - 31 October 1975).

[11] B. T. Khuri-Yakub and G. S. Kino, Electronics Letters 12, 11, 271 (27 May 1976).

[12] T. M. Reeder, W. R. Shreve, and P. L. Adams, IEEE Trans. on Sonics and Ultrasonics SU-19, 466-470 (October 1972).

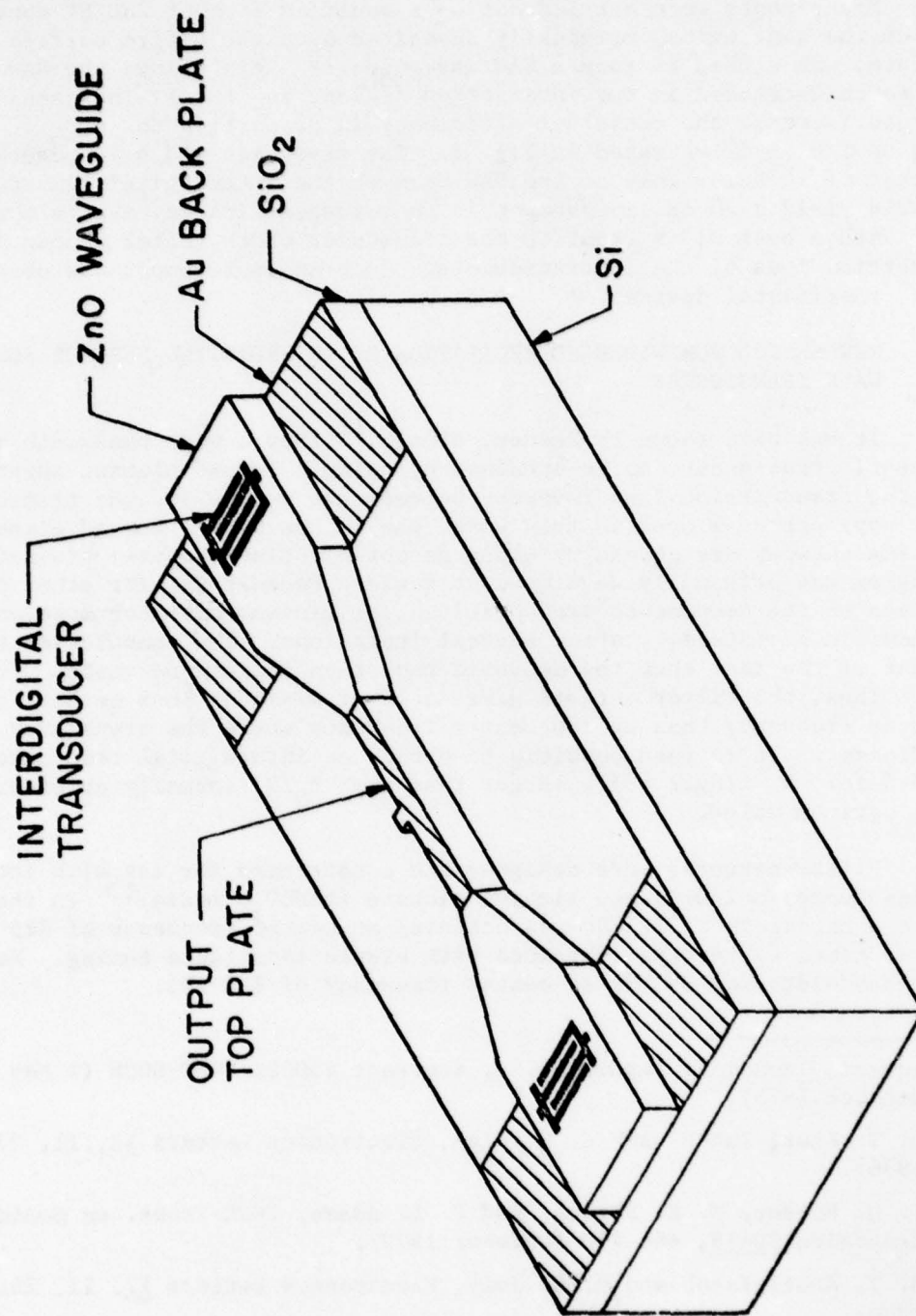[13] B. T. Khuri-Yakub and R. L. Joly, Electronics Letters 12, 11, 266 (27 May 1976).

FIG. 2—Schematic of the waveguide zinc oxide on silicon convolver.

III.   NONLINEAR BaTi AND PVF$_2$ STUDIES

Barium titanate capacitor elements and polyvinylidene fluoride films were operated as nonlinear, electrostrictive acoustic transducers. The BaTi elements showed suprisingly high efficiency. At high signal levels, the conversion efficiency was comparable to that of standard PZT elements operating as linear transducers, in the 2 to 4 MHz frequency range. This was a brief project under the contract, but one which may have future consequences for acoustic transducers and signal processing. This work is described elsehere[14,15] and will not be considered further here.

_____

[14] Interim Technical Report No. 5, Contract F30602-74-C-0038 (1 November 1975 - 30 April 1976).

[15] K. N. Bates, "A Highly Electrostrictive Ceramic," IEEE Ultrasonics Symposium (October 26-28, 1977).

IV. ANALOG-TO-DIGITAL CONVERSION USING LINEAR
SURFACE ACOUSTIC WAVE DELAY LINES

A. INTRODUCTION

With the advent of electronic computers and their associated digital
circuitry a need quickly arose to interface the analog world to the digital.
That need was met with the analog-to-digital (A/D) converter. An A/D con-
verter, or ADC, is a device which produces a digital output, a number, cor-
responding to a given analog input level. This correspondence is usually a
linear one with the output directly proportional to the input. Since the
1950's, the progress on analog-to-digital converters has advanced quickly
from the early digital voltmeters that covered a desk top to today's single
IC converters that interface directly with microprocessors.

To date, the most popular forms of A/D conversion have been the inte-
grating type and the successive approximation type. The former offers high
resolution and accuracy while the latter has high speed and fewer external
components. We have developed another type of A/D conversion technique
which uses a surface acoustic wave (SAW) delay line as an integral part of
the system. It uses a convolution property of basic two-port SAW delay lines
that has not heretofore been employed.

The new device has the potential for parallel processing with high
speed. This type of operation can be very important in cases where large
numbers of sensors are used to gather data from rapidly changing events,
which then need to be processed and displayed in real time. For example,
consider an array of high speed sensors producing simultaneous outputs which
need to be digitized for processing and then displayed on a CRT. The number
of resolution elements in the array can range from hundreds to thousands,
and if these are A/D converted sequentially, they cannot be displayed at the
usual scan rates, while parallel conversion to maintain speed requires a
very large number of A/D converters. The potential ability of the SAW-ADC
to provide parallel conversion of tens of high speed channels in a single
device could be important in applications of this kind.

B. PRINCIPLES OF OPERATION

The technique uses the impulse response of a SAW delay line to provide
a reference waveform against which the analog input is compared, the impulse
response being the output signal resulting from a voltage spike at the input.
Referring to Fig. 3(a) a rectangular voltage spike is seen to have produced
a surface wave packet propagating away from the input transducer. The
transducer produces two identical waves but only the one traveling toward
the receiving transducer is used. The other one is purposely absorbed by
attenuating material placed on that side of the transducer. As the wave be-
gins to travel underneath the output transducer, a signal is produced that
is directly proportional to the amount of the surface wave packet that is
under the output transducer at any instant. The signal increases linearly

as the packet fills the transducer and then decreases linearly as the wave leaves the other end. This process can be viewed as the convolution of the spacial shape of the traveling surface wave packet with that of the output transducer. Since the acoustic packet is produced by impulsing the input transducer, its shape will closely resemble the shape of the transducer. Therefore, the impulse response of the delay line will be closely approximated as the convolution of the two transducer patterns.

In the case of two identical constant aperture transducers, the output will be an rf waveform with a triangular amplitude envelope, as in Fig. 3(b). It is the triangular shape of the output signal that is the primary factor in the SAW-A/D conversion scheme. The point to note is that there exists a linear relatiohsnip between the location, in time, of the peak of a wave cycle and its amplitude. The A/D conversion scheme simply involves counting the number of peaks that pass until the amplitude exceeds the input analog signal level. This can be done on either the rising or falling half of the output triangle.

The primary functional blocks of this scheme are (1) the SAW delay line and associated impulse generator and amplifier, (2) a comparator - the device that decides when the SAW delay line output exceeds the analog signal, and (3) a counter - the device that counts the individual wave cycles.
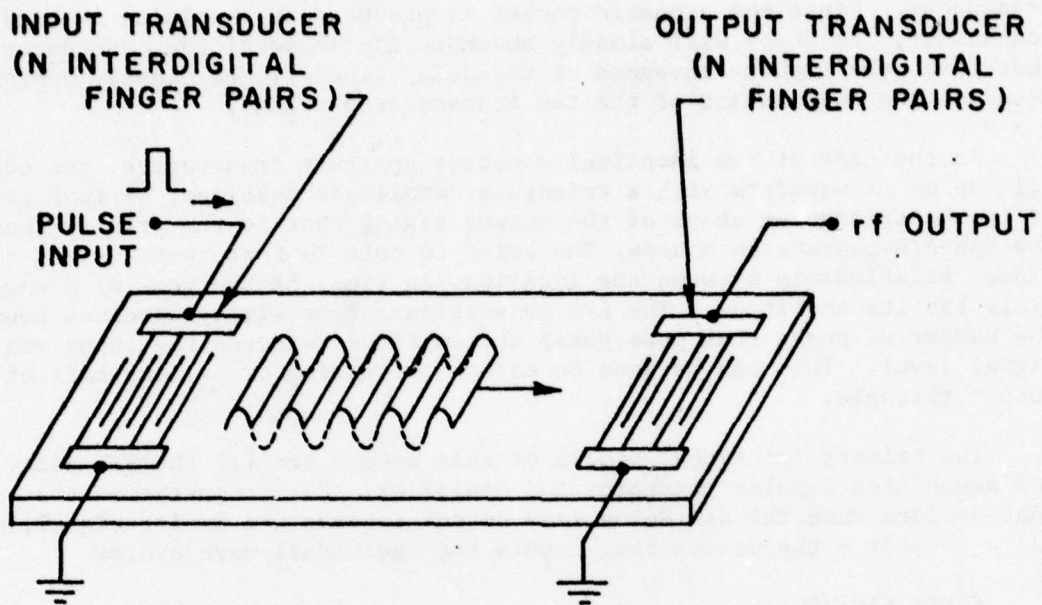
C.   FIRST SAW-ADC

A first experimental model to prove the principle of SAW A/D conversion was constructed using modest parameters. The number of bits was limited to four, and the operating frequency of the delay line, which is inversely proportional to the conversion speed as discussed later, was 52 MHz. These values simplified the design and construction of the first device, but were adequate to establish the feasibility of the scheme.
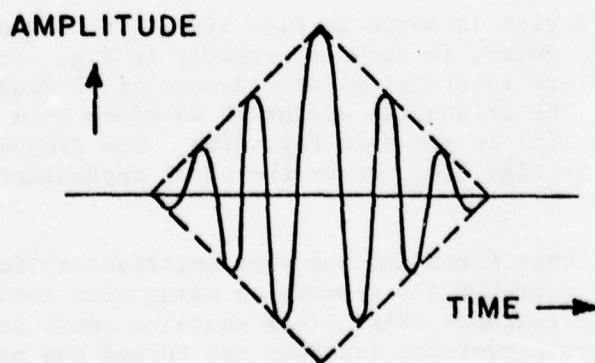
A photo of this device is shown in Fig. 4(a). The SAW delay line, located to the right of center, is shown separately in Fig. 4(b). This delay line contains two uniform interdigital transducers of 30 finger pairs on a $Bi_{12}GeO_{20}$ substrate. The triangular output rf waveform from this delay line, corresponding to Fig. 1(b) is shown in Fig. 5(b). The frequency response of the delay line, shown in Fig. 5(a), shows the usual approximate $(\sin x/x)^2$ form as expected.

The operation of this first ADC was very satisfactory for its intended purpose. It provided four-bit A/D conversion using slow readout on an array of LED's. The impulse response (Fig. 4(b)) contains small deviations from linearity, which affect conversion accuracy and formed the basis for some delay line design considerations in the later device described below. Further details on the first device and its performance are given in an earlier report[16] and will not be reported here.

---

[16]Interim Technical Report No. 3, Contract F30602-74-C-0038 (1 November 1974 - 30 April 1975).

INPUT TRANSDUCER
(N INTERDIGITAL
FINGER PAIRS)

OUTPUT TRANSDUCER
(N INTERDIGITAL
FINGER PAIRS)

PULSE
INPUT

rf OUTPUT

(a) SAW DELAY LINE SCHEMATIC.
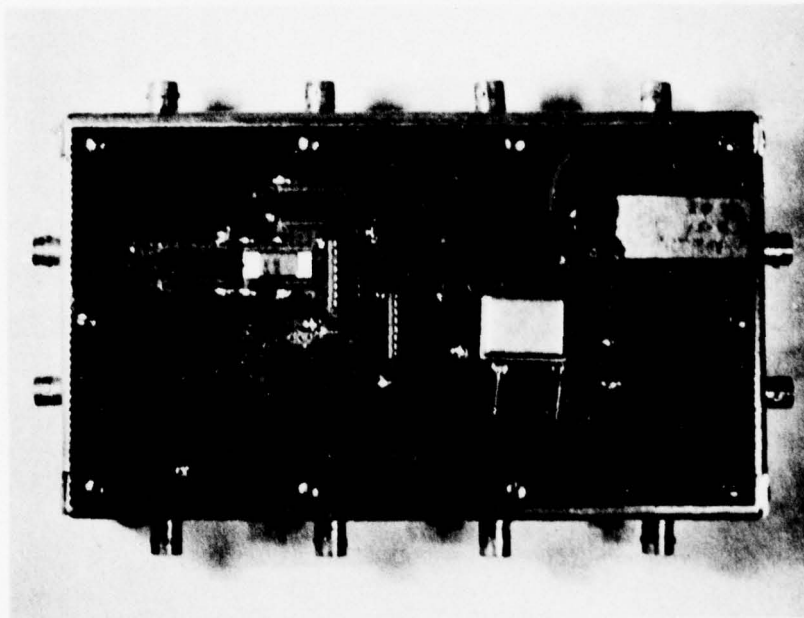
AMPLITUDE

TIME

(b) rf OUTPUT PULSE.

FIGURE 3

FIG. 4(a)--Original SAW analog to digital converter.
The metal package is the SAW delay line.
The readout consists of 5 light emitting
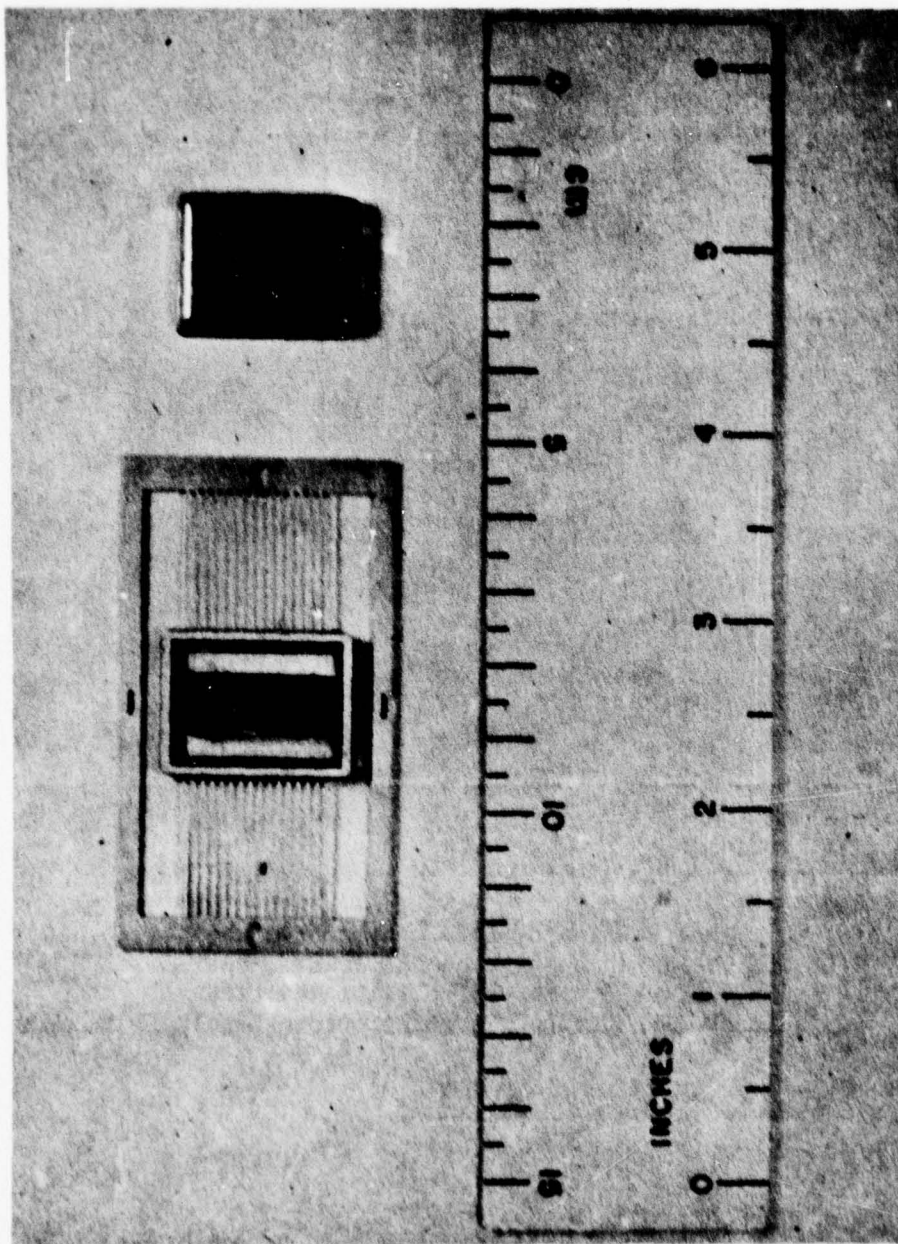diodes (on the upper right of photograph).

FIG. 4(b).--Surface wave delay line. The delay line is seen centered in a microcircuit package at the right. It consists of a polished $Bi_{12}GeO_{20}$ substrate with transducers at both ends (only the electrical bonds to the transducers are visible in this view). A closeup view of one transducer is shown in Fig. 4(c).
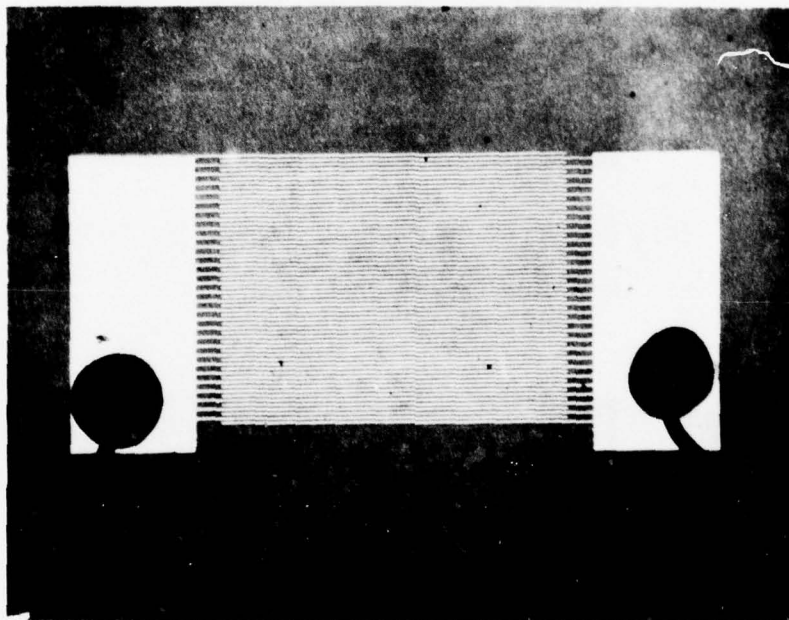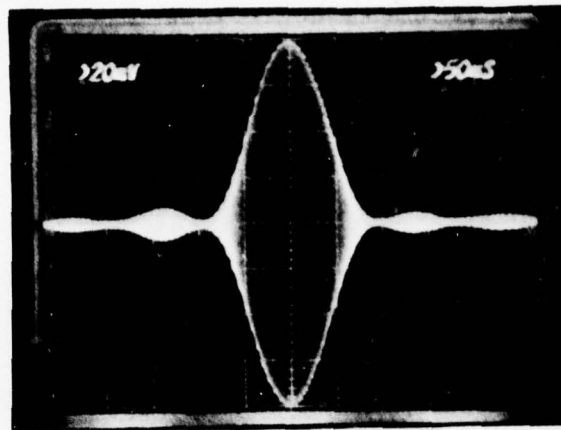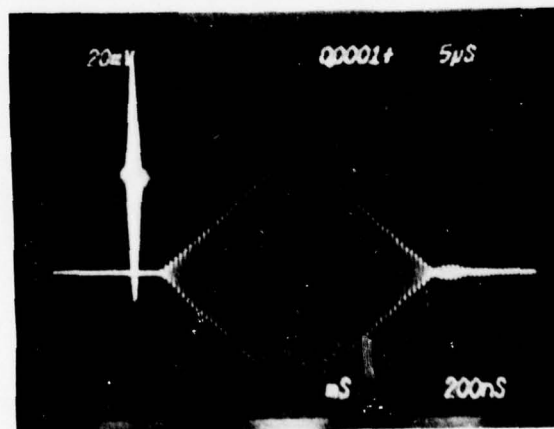
FIG. 4(c)--Closeup view of one transducer on delay line of
         Fig. 4(b). It contains 30 finger pairs of chrome/
         gold, and operates at a center frequency of 52 MHz.

(a) Frequency response of first SAW delay line used for A/D conversion. The sweep is 10 MHz wide centered at 51.27 MHz.

(b) Impulse response of the above delay line.

FIGURE 5

D.   SYSTEM COMPARISON

Once we had demonstrated the concept of the SAW-ADC, we investigated how well systems based on this principle might compare to the existing state-of-the-art of ADC's. We felt that a SAW-ADC could be built at this time with 8 bit accuracy and a 2 μsec conversion time, and that higher accuracies and speeds would be possible in the future with further engineering effort. This compared well to monolithic, silicon, 8 bit ADC's presently on the market.

Unlike many high speed techniques of A/D conversion, the SAW-A/D approach is amenable to parallel processing, as mentioned earlier. This feature may well be the most useful aspect of the method. The SAW delay line, in effect, provides the reference signal to which the analog signal is compared. It is important to note that the delay line output could be compared with a large number of analog signals at the same time. A 32 channel SAW-ADC would need 32 comparators and counters but only one SAW delay line (see Fig. 6). Such a system would exhibit a throughput (number of channels converted per unit time) 32 times greater than that of a single channel ADC. This is a departure from standard multi-channel systems which use a single high speed ADC to sequentially convert each of the many channels. In such systems, the throughput is inversely proportional to the number of channels. The SAW-ADC system, in contrast, has a throughput that is directly proportional to the number of channels. Further details on the characteristics of this technique are given in an earlier report.[17]

E.   FINAL SYSTEM

The final system was designed to convert two analog channels into their respective digital numbers with 8 bit accuracy (7 bits resolution + 1 bit sign) in ~ 2 μsec.

1.   SAW Delay Line

The SAW-A/D conversion technique requires that the SAW delay line transducers be composed of at least 2^n finger pairs, where n is the number of bits which the system can handle. This follows from the fact that the technique involves counting the number of cycles in one-half of the triangle, so that there must exist at least 2^n such cycles to resolve the input signal to one part in 2^n . If the peaks of the cycles vary strictly linearly with time, then the input signal will be resolved to an accuracy of one part in 2^n .

As the SAW delay line output is bipolar, the technique can be used to convert a bipolar analog signal with the same resolution independent of polarity. With the addition of an accurate comparator to determine the polarity of the input analog signal, the SAW-A/D conversion scheme can achieve

---

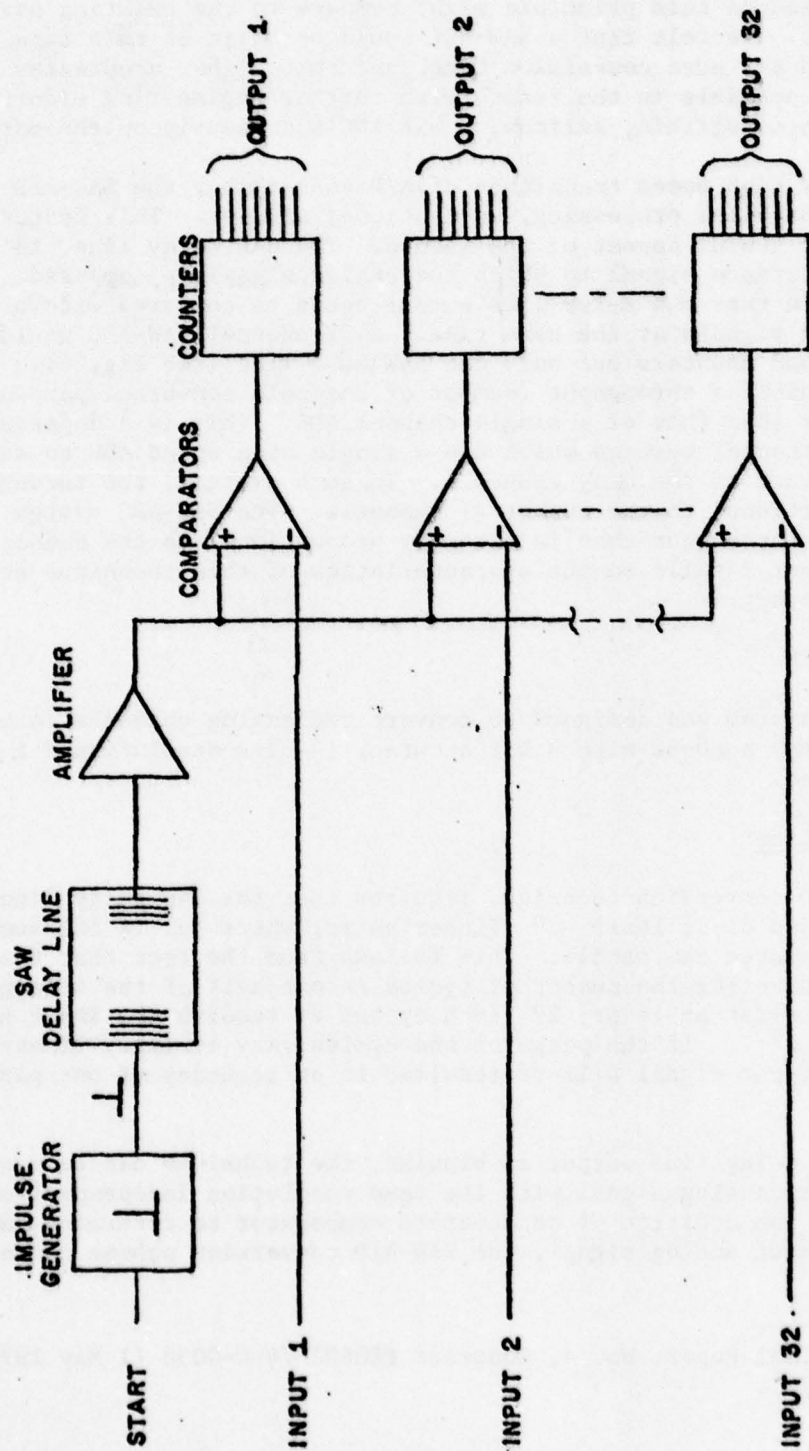[17] Interim Technical Report No. 4, Contract F30602-74-C-0038 (1 May 1975 - 31 October 1975).

FIG. 6—Block diagram of 32-channel SAW A/D converter.

an accuracy of $n + 1$ bits. Therefore, to achieve 7 bits of resolution, the SAW delay line must be composed of 128 (2^7) or more finger pairs.

The conversion time for a given resolution is determined by the center frequency of the SAW delay line.

$$t_c = 2 \cdot 2^n / f_c$$

where t_c = conversion time, n = number of bits, and f = center frequency. (The factor of 2 compensates for the dead time due to the unused half of the SAW impulse). Thus to achieve 7 bit resolution in approximately 2 μsec, the SAW delay line should operate near 128 MHz.

The original 4 bit ADC used a delay line that was not designed with our purpose in mind. Its impulse response deviated from the needed triangular one.[18] The deviations consisted of two types: (1) a small ripple of less than 1 part in 32 on the linear envelope extending over the entire span of the output triangle, and (2) a rounding of the apex of the triangle producing a maximum error of 1 part on 29. Neither of these errors is large enough to affect the accuracy of the 4 bit conversion. Computer studies[19] indicated that discrepancies of type (1) could be produced by acoustic and electric reflections from the transducer electrodes. In the design of the new delay line we took two steps to reduce these reflections, namely, the use of split finger geometry and low piezoelectric coupling constant substrates. Discrepancies of type (2) can result from wave diffraction, which can be controlled as discussed later.

The above considerations fix the number of finger pairs in the transducers and, together with the SAW velocity for the substrate material, also fix the widths and spacings of the individual fingers. The remaining parameters are the aperture, or finger length, of the transducers and the axial separation between transducers. These are also affected by properties of the substrate, namely its piezoelectric coupling coefficient, anisotropy and dielectric constant.

The transducer aperture is chosen as the best compromise between acoustic (wave diffraction) effects and electrical (capacitive) effects, both of which can lead to distortion of the impulse response. If the aperture is too small, the SAW beam profile will vary with axial position along the output transducer, due to diffraction spreading, thus altering the shape of the output triangle. On the other hand, if the aperture is too large, the interelectrode capacitance of the transducer will filter the frequency spectrum of the input electrical pulse, again causing distortion of the impulse response of the system. An electrical network might be designed which would appropriately

---

[18] Interim Technical Report No. 3, Contract F30602-74-C-0038 (1 Nov. 1974 - 30 April 1975).

[19] Interim Technical Report No. 4, Contract F30602-74-C-0038 (1 May 1975 - 31 October 1975).

match an input pulse to the characteristics of the input transducer. Calculations indicate,[20] however, that this complexity can be avoided for present purposes by proper choice of the transducer aperture and omission of any matching network between the impulse generator and the delay line.

The axial separation of the transducer should be made small. This is because increased separation of the transducers increases the effect of wave diffraction discussed above, and also introduces a time delay which constitutes an undesired dead time between successive A/D conversions. Since the delay line in this case is being used to produce filtering rather than time delay, there is no basic functional conflict in minimizing the separation. The only tradeoff involves direct capacitive rf feed through from the input to the output transducer, which is more difficult to control as the separation is reduced.

A quantitative treatment of the above design guidelines, together with details of the final transducer mask specifications, are given in the Appendix. The final delay line parameters may be summarized as follows:

Number of Finger Pairs per Transducer	140
Center Frequency	100 MHz
Substrate	ST-cut Crystal Quartz
Transducer Aperture	4992 μm
Transducer Separation	780 μm

Figure 7 is a layout of the optimum transducer design.

Figure 8(a) is a photo of a matrix of delay lines made to the above design. The IDT transducers consist of approximately 1000 Å of Aℓ deposited on a 2" X 1/2" X 1/16" ST-X quartz substrate. The propagation direction is horizontal in the figure. A complete delay line consists of any two contiguous transducers from the matrix. The upper and lower rows of transducers have different apertures, to allow experimental measurement of the effect of aperture on impulse response linearity. As will be seen from the Appendix, the transducer mask also contains other variations of transducer parameters for use in further experimentation. The deposition of a matrix of transducers as in Fig. 8(a) allows the testing of a number of transducers and selection of the most defect-free adjacent pair for the ADC. Figure 8(b) shows the delay line in its housing.
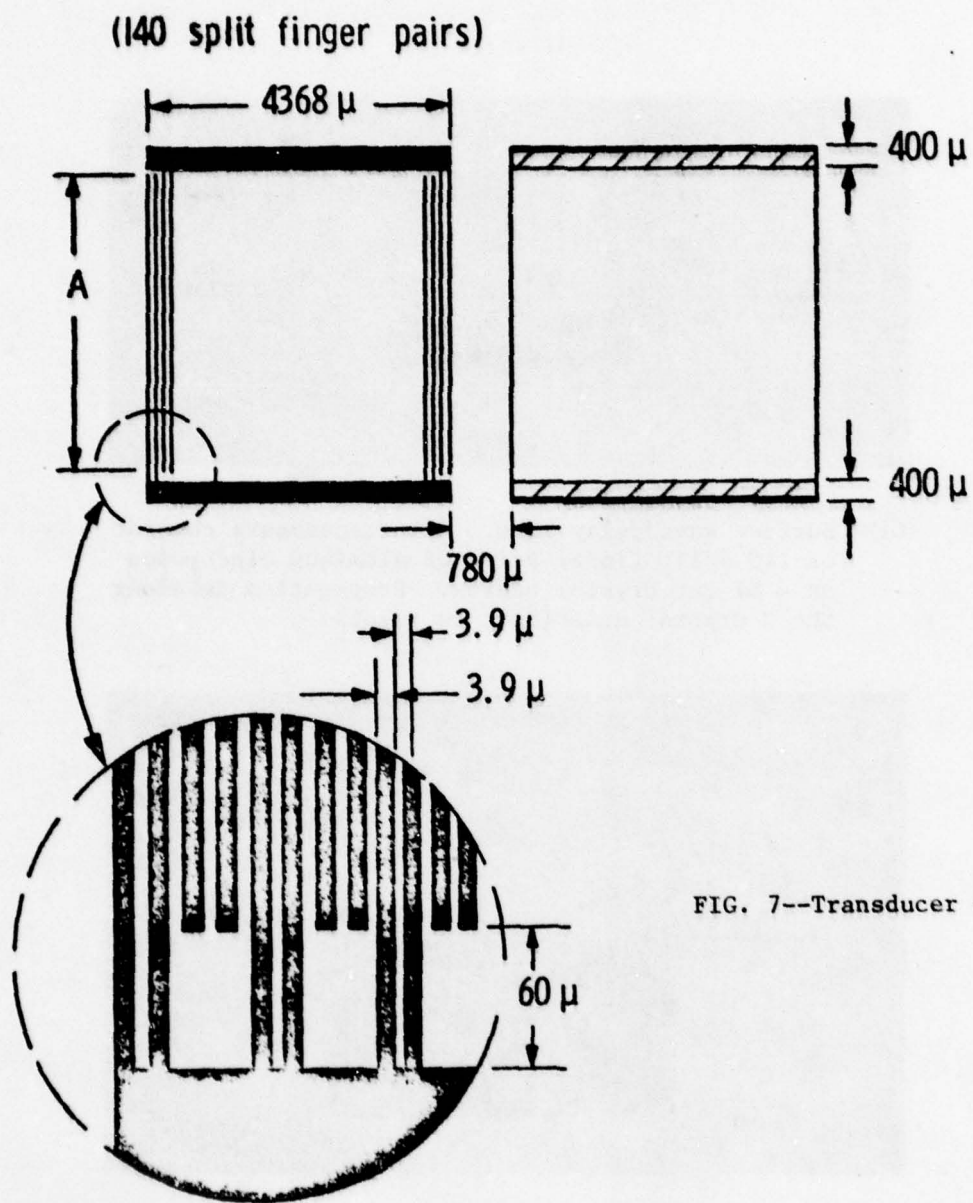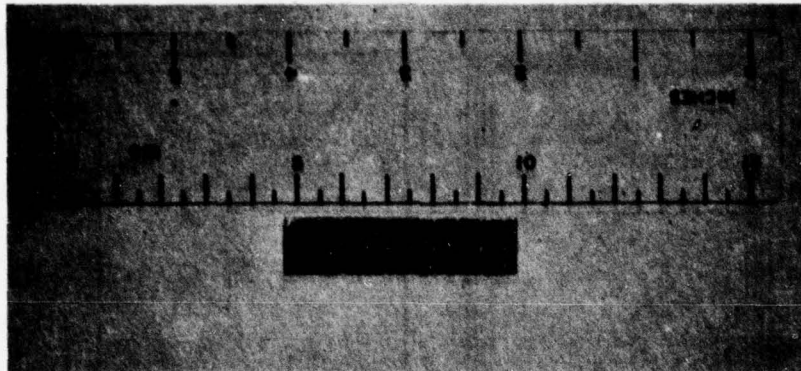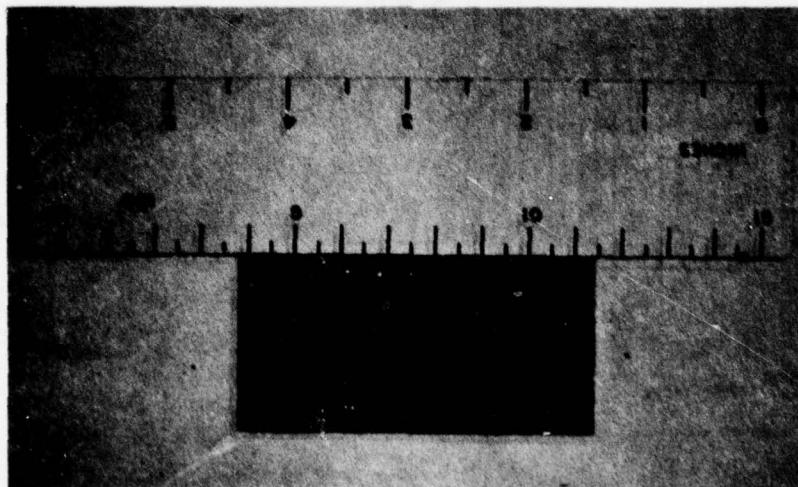

20

See Appendix A.

(140 split finger pairs)

FIG. 7--Transducer design.

- 19 -

(a) Surface wave delay line. All transducers consist of 140 split finger pairs of aluminum electrodes on a ST cut crystal quartz. Propagation is along the X crystal axis (left to right).

(b) Packaged device. The numerous connection pads allow several transducer pairs to be tested.

FIGURE 8

2. Electronic Section

With the above SAW delay line we have implemented the two channel ADC seen in Fig. 9. This system converts analog channel No. 1 into a signed 7 bit result and analog channel No. 2 into an unsigned 8 bit result. In operation, channel No. 1 accepts an unknown bipolar voltage and channel No. 2 a unipolar reference voltage. Since channel No. 2 converts a known, positive, fixed voltage, its digital output should be constant if there are no variations in the SAW delay line signal. Therefore, channel No. 2, then, can be used to measure the stability of the converter accuracy due to variation of the impulse generator output or the amplifier gain. Since both channels share the same SAW delay line and associated electronics, their digital outputs may be divided to produce a single digital result that is free of errors due to any common gain fluctuations.

When the conversion process is initiated by a pulse at the start input, the counter section is reset and the impulse generator triggered. After the input-to-output transit delay of the delay line, the triangular impulse response is amplified and inputted to the comparators. At this time, referring to Fig. 10(a), the two signals, the triangular waveform and the analog signal, are present at comparator "stop". Simultaneously, the triangular envelope and zero voltage (ground) are compared in the zero crossing comparator "0-X". Comparator "0-X" produces a digital "1" when the SAW delay line signal exceeds zero volts, otherwise its output is a digital "0" (see Fig. 10(b)). The counter counts the number of "0" to "1" transitions until the triangular wave exceeds the analog input. At that time, comparator latch produces a "1", setting a set/reset flip-flop whose output forces the latches to store the digital count at that instant (see Fig. 10(c)). The counter continues until the triangular wave exceeds the second analog or reference input. Comparator "stop" then stops the counter, thus completing the conversion process.

Figure 11 is a schematic of the digital electronics section. Notice that it is divided into four subsections: analog input, counter, control and output. Figure 12 is a photograph of this section and Fig. 13 is a map of the location of the subsections.

The control and output subsections of the electronics section interface the ADC to a microcomputer.

3. Test Bed

The SAW-A/D conversion characteristic, or transfer curve, was generated by an automated test assembly. See Fig. 14. This test bed consisted of the ADC, two 10-bit digital to analog converters (DAC's), an X-Y recorder, and a microcomputer.

In operation, the computer sends a digital signal to the X channel DAC. The DAC converts this number into the corresonding analog voltage. This analog voltage serves as the unknown input to the ADC and the X input to the recorder.
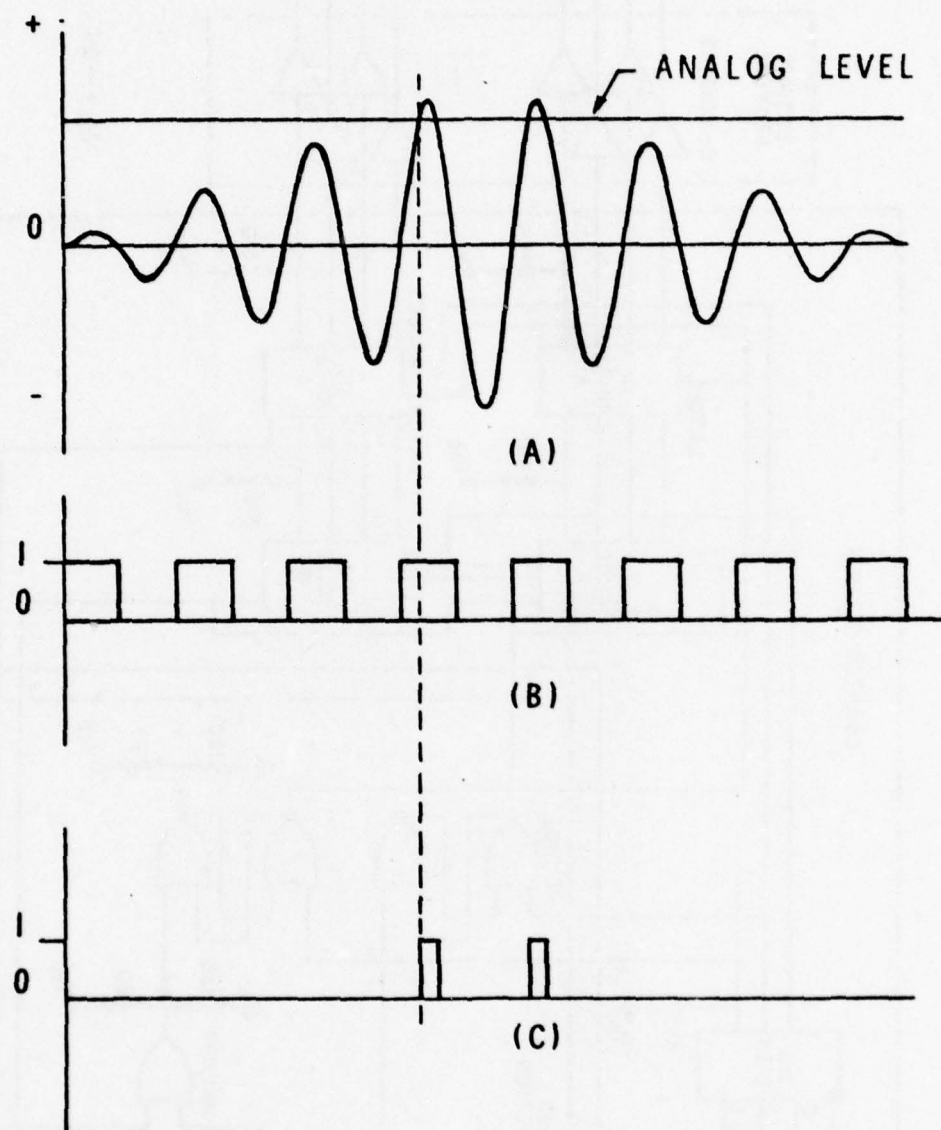
FIG. 9—Block diagram for two-channel system.

FIG. 10(a)--SAW delay line and analog signals.
    (b)--Output of zero crossing comparator.
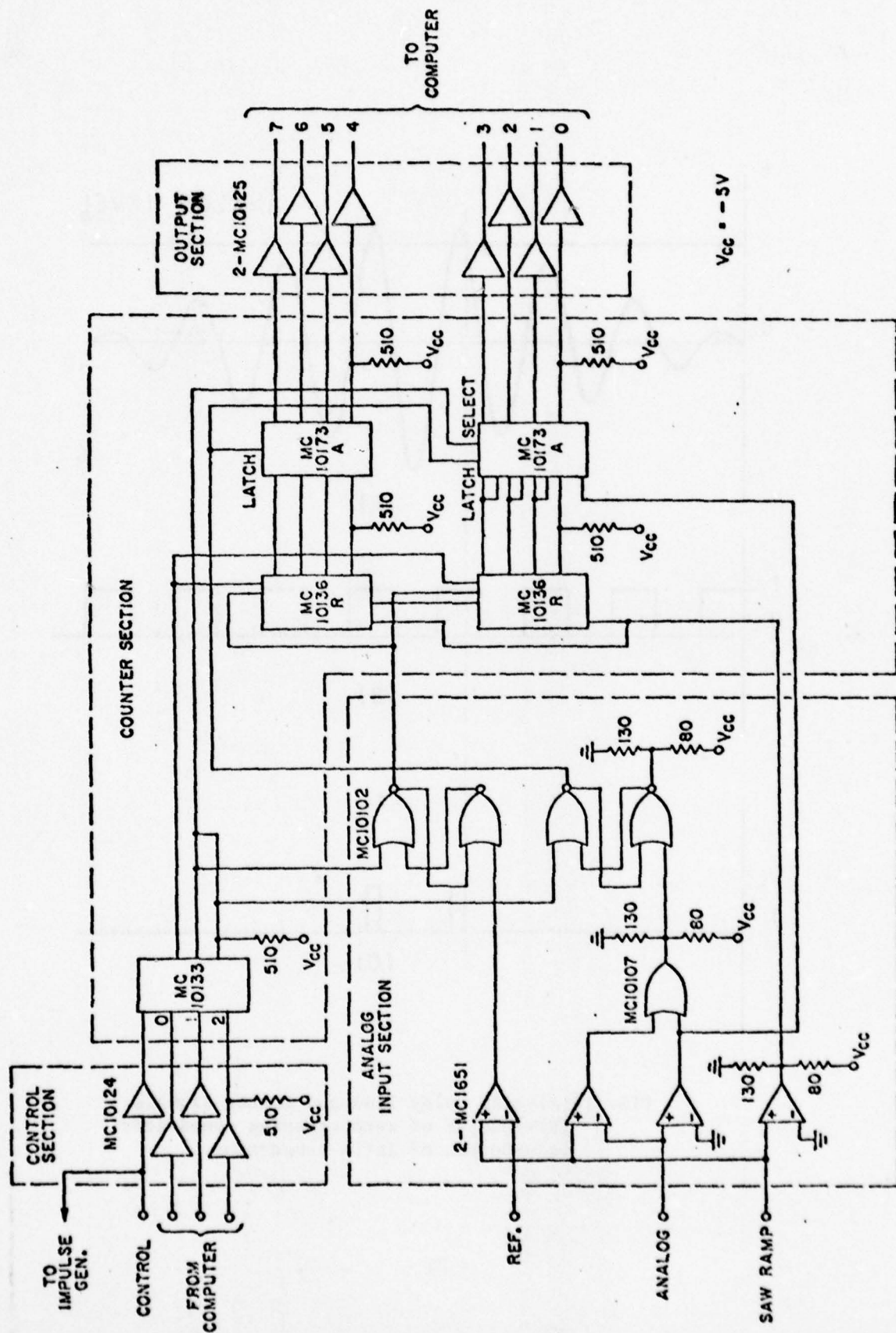   (c)--Output of latch comparator.
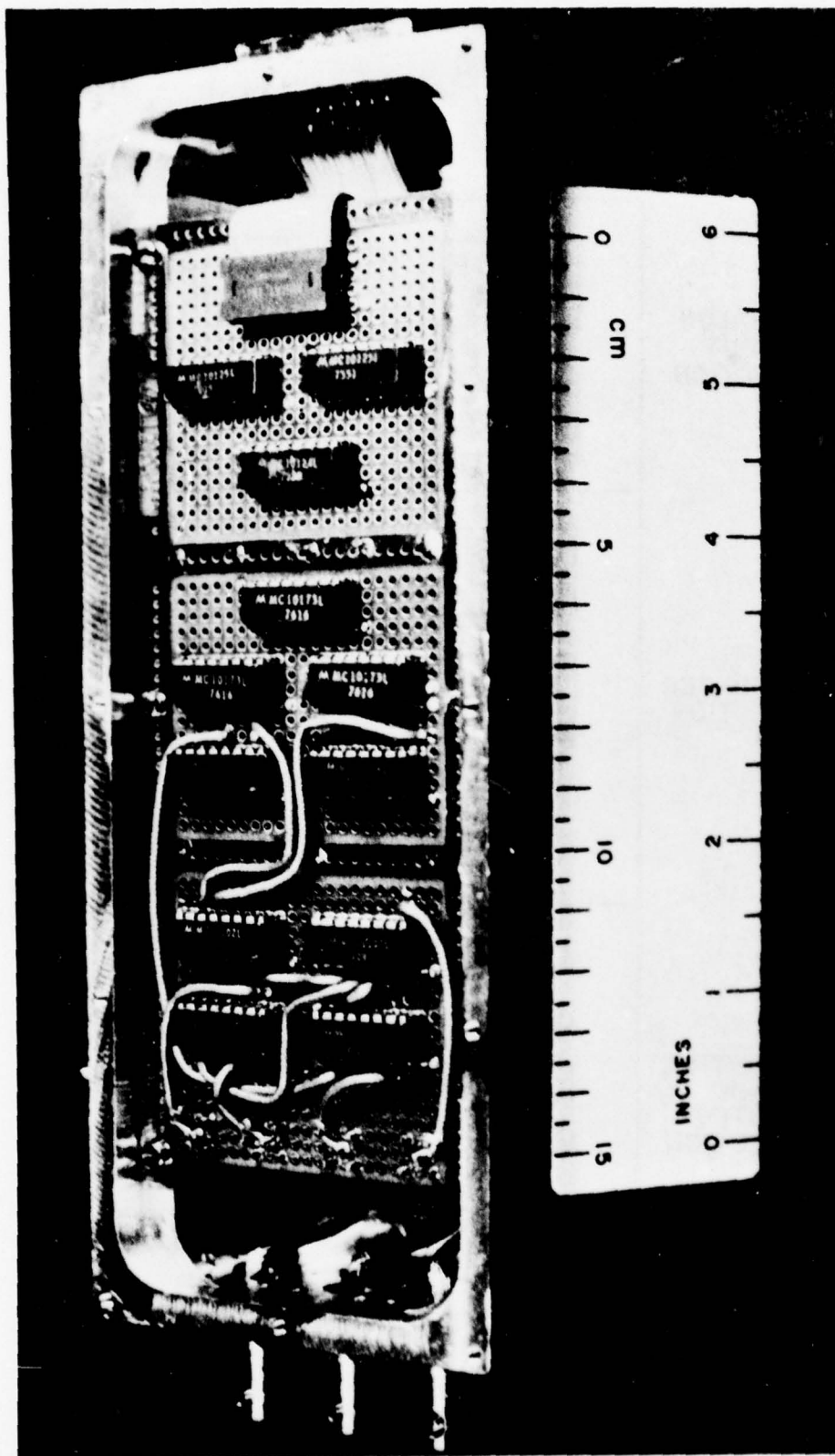
- 23 -

FIG. 11--Schematic of the electronics sections.
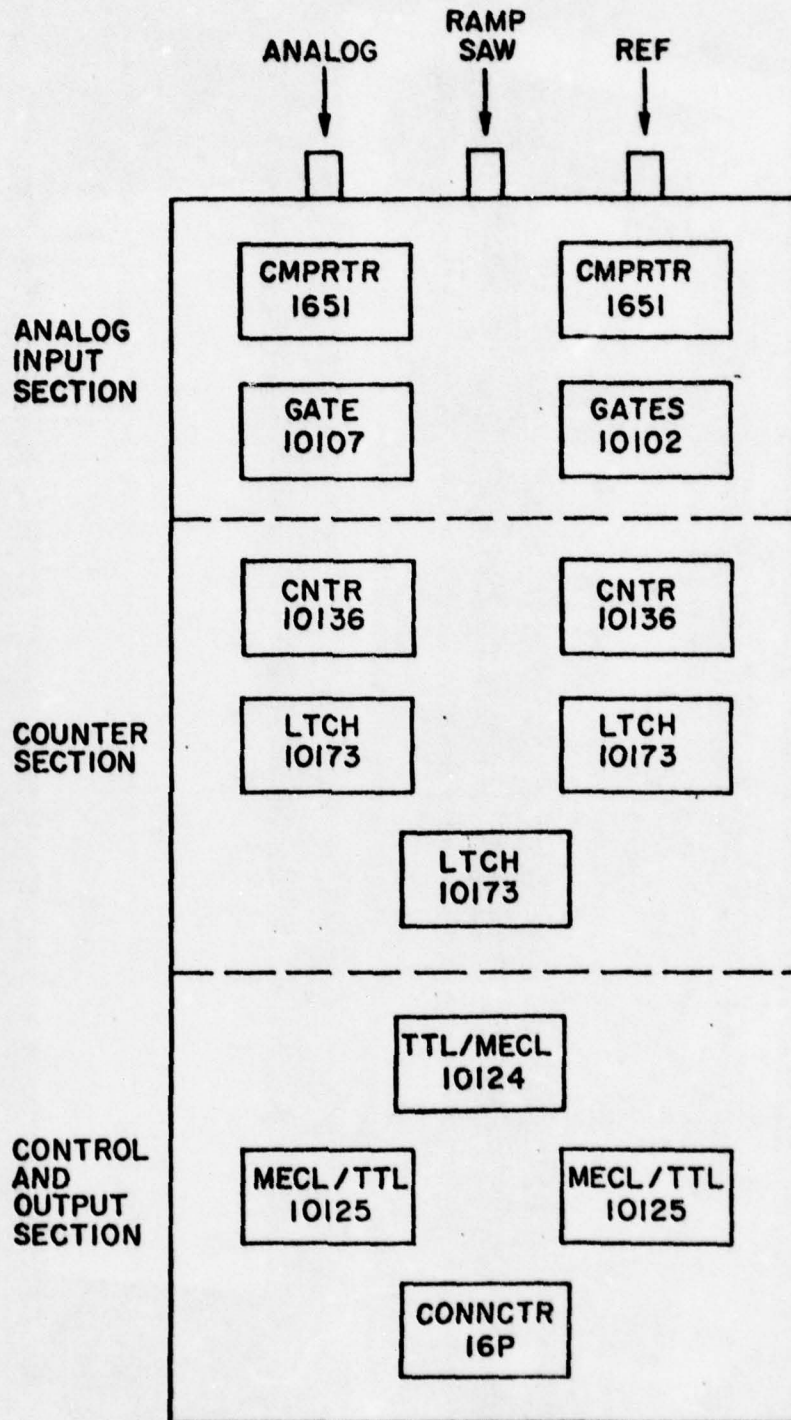
FIG. 12--Electronics sections of 8-bit SAW-ADC.

FIG. 13--Layout of sections in the device.

RECORDER

DIGITAL

DAC

ANALOG   Y

DAC

COMPUTER

ADC

X

CONTROL

DIGITAL

(a)

Subsystem Breakdown

IMPULSE
GENERATOR

SAW
DELAY
LINE

CONTROL

ELECTRONICS

ANALOG
INPUT

REFERENCE
INPUT
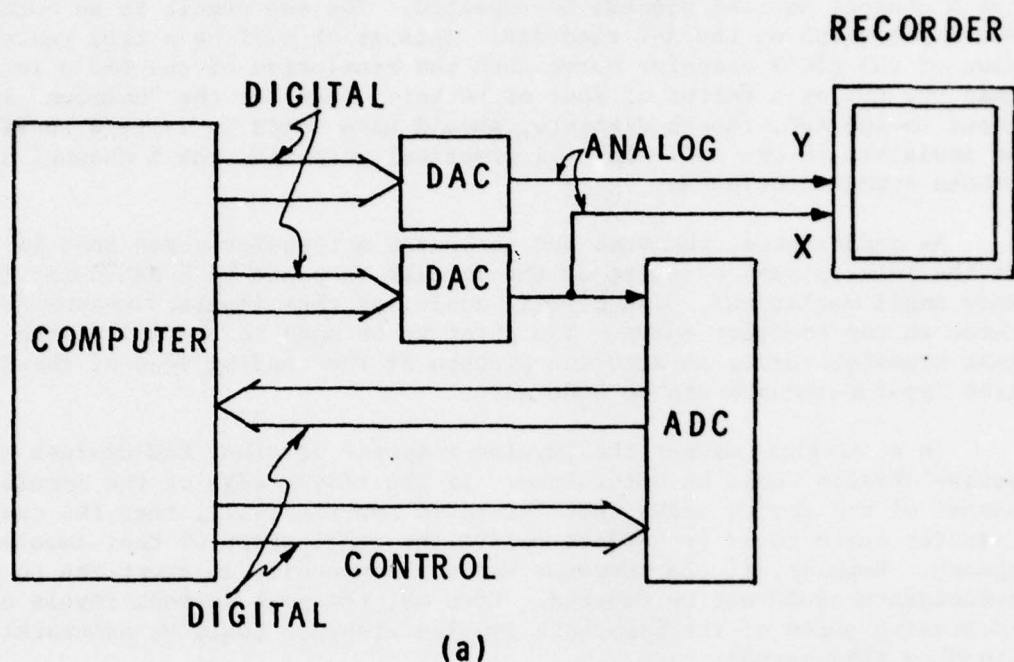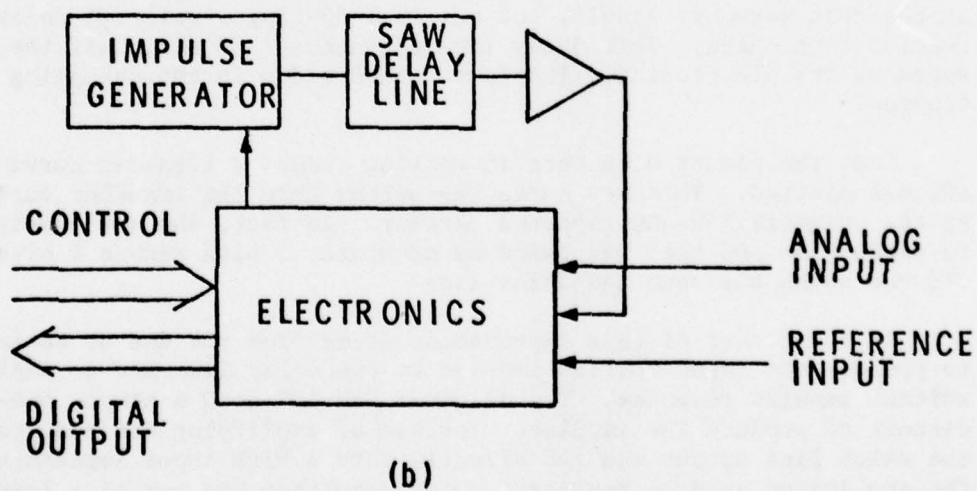
DIGITAL
OUTPUT

(b)

Components of SAW-ADC Subsystem

FIG. 14--System for testing of SAW-ADC.

- 27 -

At this point the computer sends a control signal to the ADC to convert the "unknown" signal. The digital output of the ADC is fed back into the computer and from there into the Y channel DAC. The computer then increments the X channel and the process is repeated. The end result is an output versus input graph on the X-Y recorder. This graph will be a true representation of the ADC's transfer curve when the resolution of the DAC's is greater than the ADC by a factor of four or better. That is, the "unknown" analog input to the ADC, though discrete, should have steps in voltage so fine as to be invisible to the ADC. For all practical purposes, the X channel signal should appear continuous.

As constructed, the test bed generates a transfer curve that is related to the peak to peak envelope of the impulse response of a SAW delay line. Very small variations, 0.4% of full scale, of that impulse response are captured in the transfer curve. The point to be made is that given the resultant transfer curve, an accurate picture of the leading edge of the SAW delay line impulse response can be deduced.

In a similar manner the impulse response of other SAW devices or even active devices could be determined. If the rising edge of the impulse response of the device under test increased monotonically, then the resultant transfer curve could be used to derive the exact shape of that impulse response. However, if the response was not monotonic, an exact one to one correspondence could not be deduced. Even so, the peak to peak levels of the increasing parts of the monotonic impulse response could be accurately determined by this method.

a. Testing of ADC with Original SAW Delay Line

As a first check on the performance of the new ADC electronics as well as the test assembly itself, the original 30 finger pair IDT delay line of Section C was used. This delay line operated at 50 MHz, half the designed speed of the electronics. The lower speed aided in the debugging of the electronics.

Once the electronics were in working order, a transfer curve of the SAW-ADC was plotted. This new curve was better than the transfer curve produced by the original SAW-ADC reported earlier. In fact, the new electronics helped to produce an ADC that was twice as accurate, 5 bits versus 4 bits, than the old one using the same SAW delay line.

At least part of this improvement stems from the use of better equipment to produce the input voltage impulse to the delay line and to amplify the resultant impulse response. The original SAW-ADC used a simple one-transistor circuit to produce the impulse. Instead of amplifying the resultant signal, the delay line output was fed directly into a high input impedance comparator. The new design used an amplifier which permitted the use of a lower impedance (50 Ω) comparator which proved to be a better device. Secondly, the use of a General Radio pulse generator permitted much better control over the pulse

shape that was inputed to the SAW delay line. Due to the 50 Ω output impedance, transmission line matching with standard cable was possible. Standard methods of electrically matching SAW delay lines proved unacceptable early in the SAW-ADC program. While optimizing the passband and insertion loss characteristics of the SAW delay line, these methods interfer with the impulse response of the device by causing out of band distortion and even ringing.

Transmission line matching, on the other hand, produced far better results than discrete devices. This was particularly true in matching the delay line to the pulse generator. This seems to point out that the smoother phase and amplitude response of transmission line matching (as a function of frequency) is particularly important to matching the wide bandwidth pulse from the pulse generator to the narrow band SAW delay line. The same beneficial effect is not seen in matching the delay line to the amplifier. The nonlinear response that is responsible for this fact probably originates in the pulse generator's output stage.

The end result was a SAW-ADC with a transfer curve accurate to 5 bits. Referring to Fig. 15, the curve is shown to fall on or within the two lines representing a $\pm$ 1 LSB error. The $\pm$ ½ LSB lines denote the error that results from quantizing alone. Error that results in the departure of the transfer curve from within the $\pm$ ½ LSB bound is known as the linearity error. This error is in addition to the quantizing error. Thus, the $\pm$ 1 LSB accuracy of the ADC can be broken down into a $\pm$ ½ LSB quantizing error and a $\pm$ ½ LSB linearity error.

b. Testing of ADC with New SAW Delay Line

Once the system was operating consistently and reliably, the new 100 MHz SAW delay line was substituted for the old delay line. There had been difficulties associated with fabrication of the 100 MHz delay line. Although the specifications on the transducer finger widths, spacings and aperture (see Section E1 above and Appendix A) are well within current IDT technology and do not constitute a basically difficult mask fabrication problem, difficulties were encountered. Part of the difficulty was concerned with long delivery delays, exaggerated by the need to reject the first set of masks, and part was concerned with substandard quality in the final set of masks. As shown below, the final delay line suffered from a number of open-circuited fingers, and there was both insufficient time to fabricate more delay lines and low probability of achieving significantly better results without new masks. However, as shown below, it was possible to verify the operation of the ADC, and to establish good correspondence between theory and practice, by operating over restricted portions of the delay line characteristics.

The best delay line that was constructed had numerous broken fingers in both transducers. The effect of the broken fingers on the impulse response of the delay line can be seen in the photo in Fig. 16. As stated in Appendix B, any error in the IDT's of the SAW delay line will produce an error in the ADC's transfer curve. The most common faults in SAW-IDT's are shorts (fingers shorted together) and opens (fingers, or portions of fingers, electrically disconnected from the buss pads).
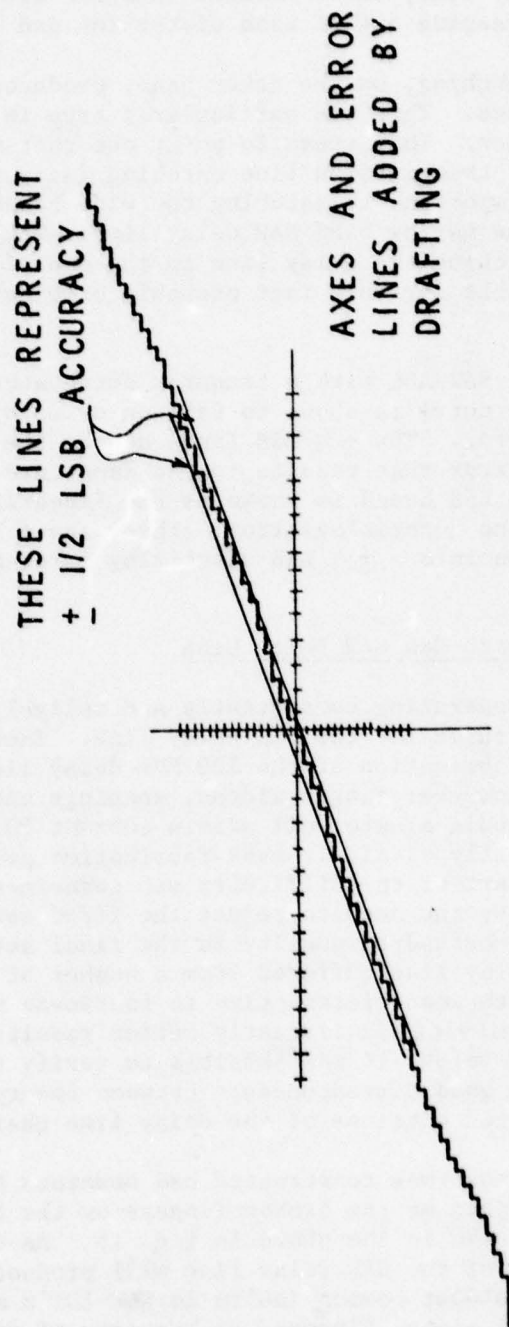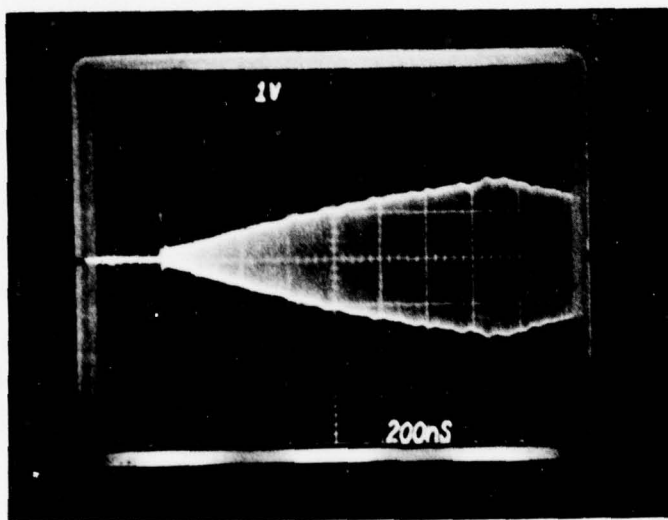
FIG. 15--Experimental transfer curve.

FIG. 16--SAW delay line impulse response.

In the SAW-A/D conversion scheme, shorts cannot be tolerated as they preclude operation of the delay line. Open circuited fingers can be tolerated, although the ADC's accuracy will be degraded. For the case of open fingers in one of the IDT's, the effects are easy to determine. For high resolution SAW-ADC's, approximately $\pm$ 1 LSB of linearity error is introduced for every missing finger. One open finger in the IDT of an 8 bit SAW-ADC would result in a device linear to $\pm$ 1 LSB, or $\pm$ 0.4% of full scale. By convention, an N bit ADC linear to $\pm$ 1 LSB is said to be linear to N bits. Therefore, providing that a perfect delay line produced a SAW-ADC accurate to $\pm$ ½ LSB (quantizing error), implying no linearity error, one open finger could be tolerated in an N bit SAW-ADC linear to N bits. Two open fingers would reduce the linearity of an N bit SAW-ADC to N-1 bits, four open fingers would reduce the linearity to N-2 bits, and so on. It should be remembered that an N-2 bit ADC is four times less accurate than an N bit device as the number of bits is $\log_2$ of the relative accuracy. As opposed to the above case where open circuits are limited to just one IDT, the effects which open fingers in both IDT's have on the accuracy of a SAW-ADC cannot be readily determined. The SAW-ADC transfer curve is directly related to the delay line impulse response, and the impulse response is directly related to the convolution of the two IDT patterns. If both IDT patterns have open fingers, the resultant convolution will produce a third pattern (the impulse response) that depends on the number and position of the open fingers in each IDT. Therefore, the number of open fingers alone does not provide enough information to precisely determine the impulse response of the delay line and hence the transfer curve of the ADC. However, the magnitude of the variation of this curve from an ideal ADC transfer curve, i.e., the accuracy, can be estimated from the impulse response of an actual imperfect delay line.

The approximate linearity error of a SAW-ADC utlizing an imperfect delay line will be the peak to peak variation of the leading edge of the impulse response from a straight line, divided by the peak level attained at the apex of that impulse response (see Fig. 17). The ($\pm$) results from the fact that the ripple is also present on the lower edge of the impulse response.

The SAW delay line used had a peak to peak variation of 0.2 volts and an apex level of 1.7 volts. The expected maximum ADC linearity error introduced is thus $\pm$ 12%. The rather large peak to peak variation was due to the 20 or so missing fingers on the IDT's of the delay line used. As a rule, the worst case peak to peak ripple introduced by a delay line with open fingers on both IDT's will be that of a delay line with the same number of open fingers on only one transducer. Therefore, the new delay line could be expected to have a worst case peak to peak ripple of 14% (20 open fingers/140 fingers). The measured ripple was 12%.

Fortunately, a portion of the impulse response did not have a great deal of ripple. As can be seen from the map of the IDT's, Fig. 18, the first portion of each transducer that faces the other is relatively free of open fingers (there were 8). The resultant fraction of the impulse response that represents the overlap of these regions would be expected to be relatively free of ripple. Indeed, the measured ripple was ˜ 2% of full scale. The resultant
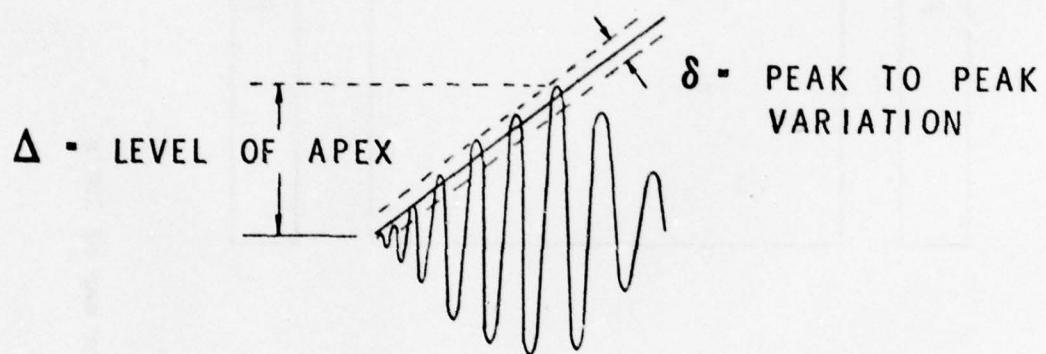
Δ - LEVEL OF APEX

δ - PEAK TO PEAK VARIATION

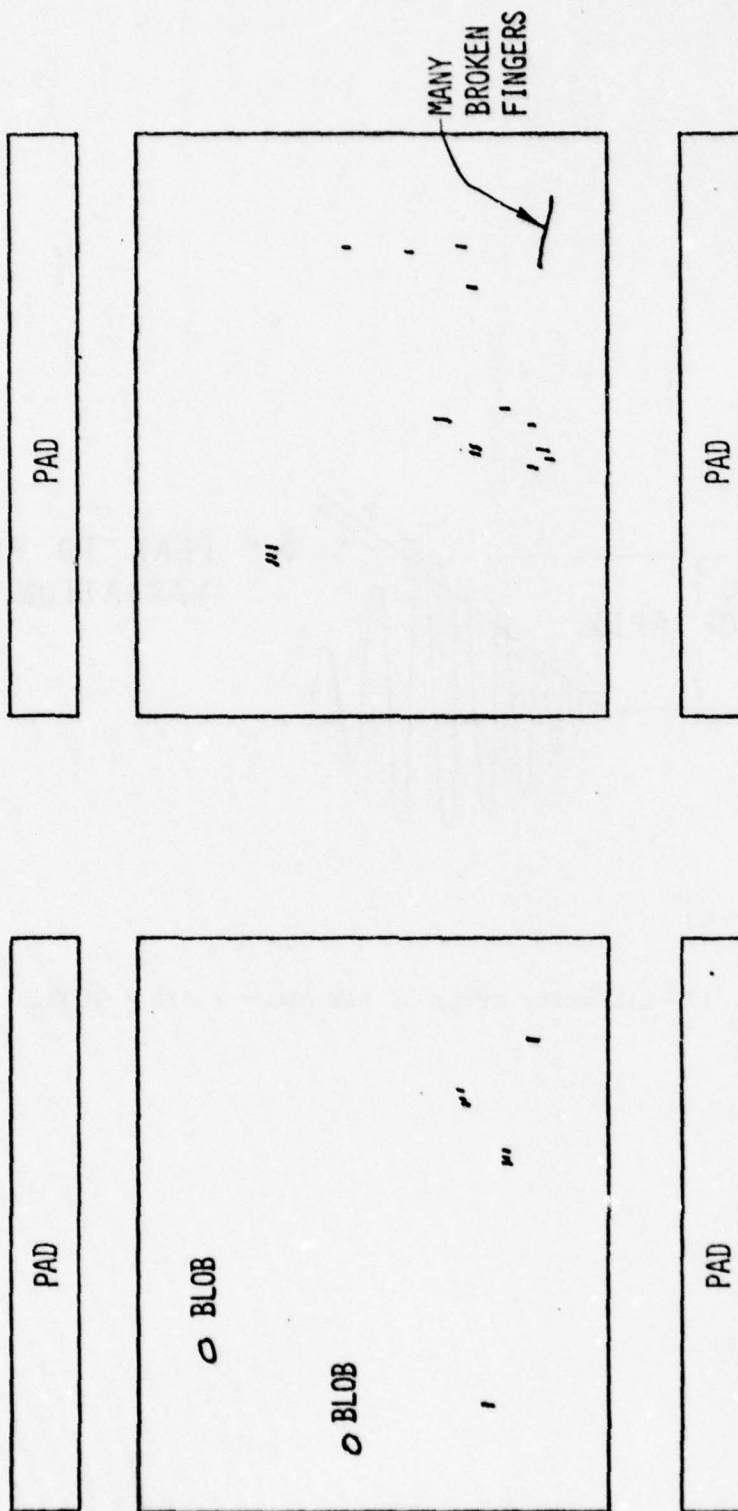FIG. 17--Linearity error of SAW-ADC $\simeq \pm\ \delta/\Delta \cdot 100\%$.

FIG. 18--Open finger map of IDT's.

ADC linearity error expected would be $\pm$ 2% resulting in an ADC linear to 6 bits over this region.

Figure 19 is a portion of the transfer curve obtained with the new delay line. The curve falls considerably outside the two lines representing the $\pm$ 1 LSB error of an 8 bit ADC. However, the curve does fall within the lines representing the $\pm$ 1 LSB error of a 6 bit ADC. Therefore, this ADC can be described as an 8 bit ADC accurate to 6 bits.

Other problems in the operation of the SAW-ADC were also encountered. Fortunately, simple solutions for these were quickly found. Two of the problems were design related and hence worth of note. The first was caused by electromagnetic feedthrough of the electrical pulse used to impulse the delay line. This EM feedthrough in the delay line was approximately 70 dB down from the input level. The 70 dB gain of the output amplifiers brought this signal back up to a level of about 6 volts. The ADC, as designed, would not respond to a feedthrough pulse of an amplitude less than 5 volts. Provisions were included to inhibit the comparators for the short period of time that the feedthrough pulse would be present. Unfortunately, this feedthrough spike was greater than the designed input limits of the comparators. As a result, this spike caused the comparators to produce an erroneous output signal that terminated the conversion process before it began. Thus, while the present feedthrough level would be acceptable for many delay line applications, it was found to be excessive for the present application. It is known that measures exist, involving shielding electrodes around and on the delay line, which could reduce this feedthrough by some 20 dB or more below its present level, and this could be done in future devices. For the present, however, there was not time to institute such measures, and a simple alternative was used. It was found possible to gate the feedthrough pulse out of the signal by the use of a fast rf switch. The second problem was erratic operation of the SAW-ADC once the EM feedthrough was eliminated. This difficulty was traced to the operation of the digital IC's responsible for counting the number of cycles in the SAW delay line impulse response. Effectively, one of the counter IC's responded too slowly to the changing logic levels. The defective IC was replaced and the ADC then operated as designed. The point to note is that the ADC failed to operate due to an IC that operated 0.5 ns slower than the manufacturer's specification. This says that the MECL 10,000 family of IC's is just barely fast enough to do the job in the 100 MHz SAW-A/D conversion scheme.

c. Test Bed Versatility

An interesting point as to the versatility of the ADC test bed can be made. It should be applicable to the testing of a wide range of devices. As presently used, the test bed generates a transfer curve that is related to the peak to peak envelope of the impulse response of a SAW delay line. Very small variations, 0.45% of full scale, of that impulse response are captured in the transfer curve. The point to be made is that given the resultant transfer curve, an accurate picture of the leading edge of the SAW delay line impulse response can be deduced.

AXES AND ERROR LINES ADDED BY DRAFTING

THESE LINES REPRESENT $\pm$ I LSB ACCURACY FOR 8 BIT ADC

THESE LINES REPRESENT $\pm$ I LSB ACCURACY FOR 6 BIT ADC
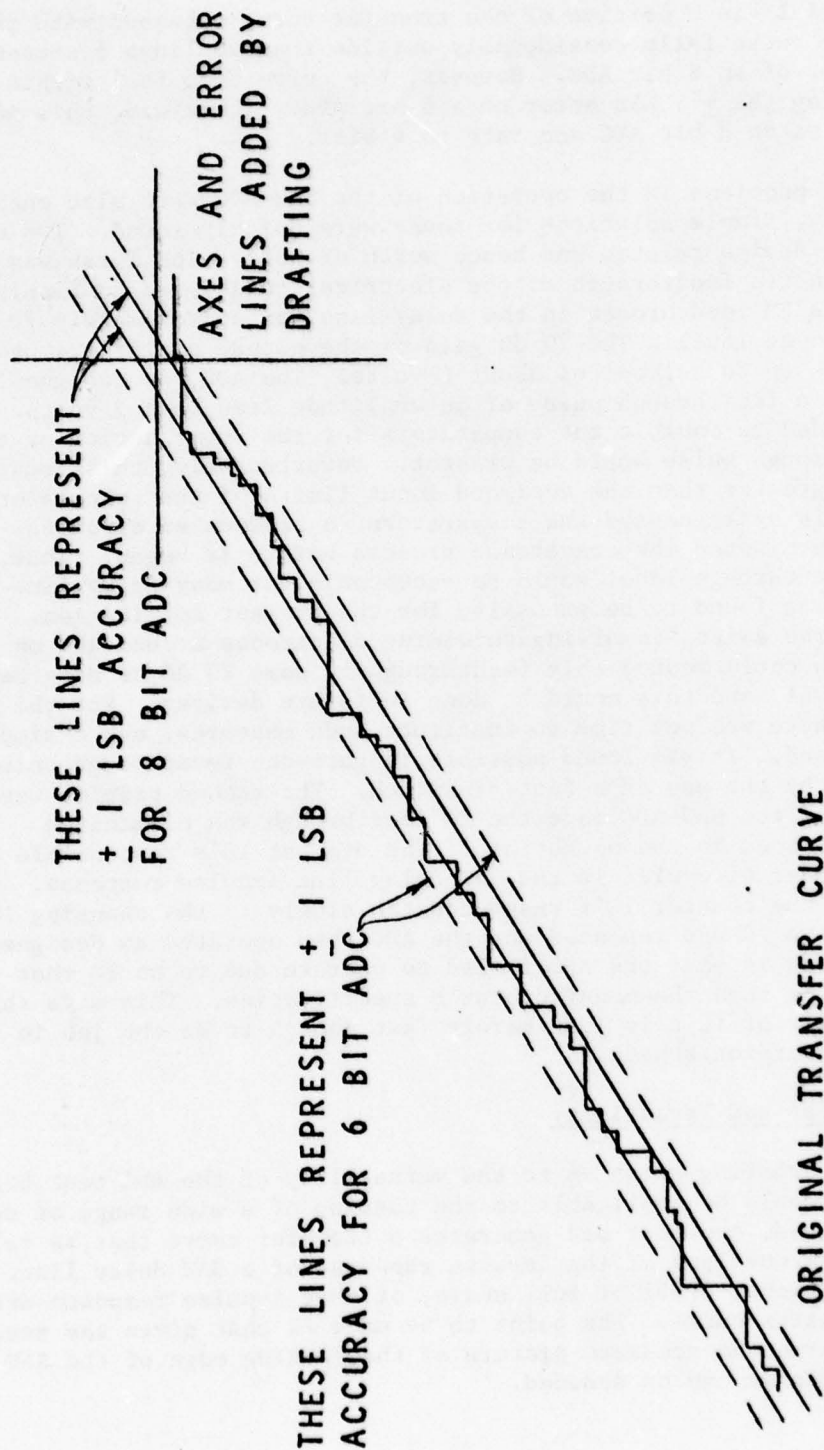
ORIGINAL TRANSFER CURVE

FIG. 19--Segment of transfer curve of 100 MHz delay line.

In a similar manner the impulse response of other SAW devices or even active devices could be determined. If the rising edge of the impulse response of the device under test increased monotonically, then the resultant transfer curve could be used to derive the exact shape of that impulse response. If the response was not monotonic, an exact one to one correspondence could not be deduced, however, the peak to peak levels of the increasing parts could be accurately determined.

APPENDIX A

DESIGN OF SAW DELAY LINE

The objective is to make a 7 bit A/D converter operating at around 100 MHz. Therefore, 2^7 (128) pairs of fingers are minimum. To give some leeway, it was decided that 140 pairs be made.

For reasons to be given below, ST-X quartz is the best candidate as a substrate. Therefore, all design parameters are calculated with quartz in mind. For example, to determine the acoustic wavelength, we divide surface velocity of quartz, 3158 m/s, by 100 MHz and get 31.58 micron.

Therefore, N = 140 and λ = 31.58 μ are taken as given. The remaining variables are aperture and distance between transducers, which in turn depends on the substrate properties such as coupling coefficient, power flow angle, propagation loss, and capacitance per unit length. In our scheme of A/D conversion, we want <u>minimum nonlinearity in the output triangle and minimum acoustic dispersion</u>.

Departure from absolute linearity is due primarily to reflection of acoustic waves by the fingers and propagation loss.

1. Finger Reflection

High coupling constant, which reduces insertion loss also gives rise to high finger reflections. In the present application, it was felt that sufficiently low insertion loss could be obtained with low coupling coefficient, which eases the problem of obtaining low finger reflections. Among the most popular SAW substrates, $LiNbO_3$, $Bi_{12}GeO_{20}$, and quartz, ST-X quartz gives the lowest coupling constant of 0.0016 (as measured by Schulz and Matsinger, 1972).

Finger reflections can be further reduced by using <u>split fingers</u>, which generate reflected acoustic waves that are 180° out of phase with each other, and therefore interfere destructively. Therefore, finger width is $\lambda/8$ = 3.9 μ .

2. Mass Loading

This effect can be minimized by going to the lighter electrode metals. Therefore, aluminum fingers are preferred to gold fingers.

3. Diffraction

Diffraction is an intrinsic property of wave propagation. The extent of diffraction is determined by the slope of the power flow angle $(\gamma = \partial\phi/\partial\theta)$, which differs from one substrate to another.

The exact diffraction theory is extremely intricate, therefore we use the parabolic diffraction theory, which was developed by Cohen[A.1] and Szabo and Slobodnik.[A.2] Cohen showed that when the velocity anisotropy near pure-mode axes can be approximated by a parabola, the diffraction integral reduces to Fresnel's integral with the following change:

$$\hat{Z} = \hat{z} \, |1 + \gamma|$$

where $\hat{z} = Z/\lambda$, Z = distance from transducer, λ = acoustic wavelength, $\gamma = \emptyset/\gamma\theta$.

A computer program was written to calculate the effect of diffraction of the propagating wave. Summing up the waves intercepted by the fingers of the output transducer, we can get the output signal. This signal would be slightly curved due to diffraction; the extent of curvature depends on the transducer aperture, the wavelength, and the distance between input and output transducers. The general shape of the output signal is as shown in Fig. A.1. A straight line of constant slope represents the ideal output. The greatest departure from this straight line (δ_{max}) represents the maximum error. This has to be smaller than 1/2 least significant bit if our system needs to have an accuracy of one bit.

This δ_{max} is plotted in Fig. A.2, with three different distances (D) between transducers (0, $25A$, 50λ) and varying apertures (A). It can be seen from the graph that for $D = 0\lambda$, $A > 112\lambda$, for $D = 25\lambda$, $A > 144\lambda$, and for $D = 50\lambda$, $A > 170\lambda$.

To separate the rf feedthrough from the desired signal, a large D is favorable, but this in turn requires a larger aperture which is more difficult to fabricate and has larger capacitance. We choose a compromise of 25λ.

Similar calculations for $LiNbO_3$ and $Bi_{12}GeO_{20}$ were done with $D = 25\lambda$, and these are displayed in Fig. A.3 and Fig. A.4 respectively. It should be pointed out that for a YZ $LiNbO_3$, with $\gamma = -1.083$ the parabolic theory is not a good approximation. Therefore, this calculation cannot be taken literally; it can only serve as an indication.

From Fig. A.3, we seen that for YZ $LiNBO_3$, $D = 25\lambda$, A can be as small as 40λ . For $LiNbO_3$, $A > 96$. From Fig. A.4, for $Bi_{12}GeO_{20}$, $A > 180\lambda$.

Therefore, if we use $Bi_{12}GeO_{20}$, $LiNbO_3$ and quartz, the minimum acceptable apertures would range from 40λ to 144λ ($D = 25\lambda$).

[A.1] M. A. Cohen, "Optical Study of Ultrasonic Diffraction and Focusing in Anisotropic Media," J. Appl. Phys. 38, p. 3821-3828 (1967).

[A.2] T. L. Szabo and A. J. Slobodnik, Jr., "The Effect of Diffraction on the Design of Acoustic Surface Wave Devices," IEEE Trans. Sonics and Ultrasonics SU-20, p. 240-251 (1973).
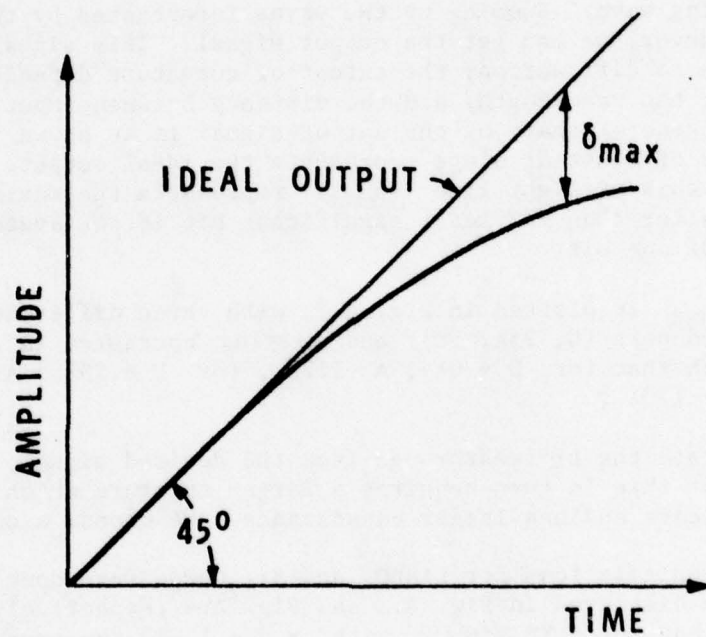
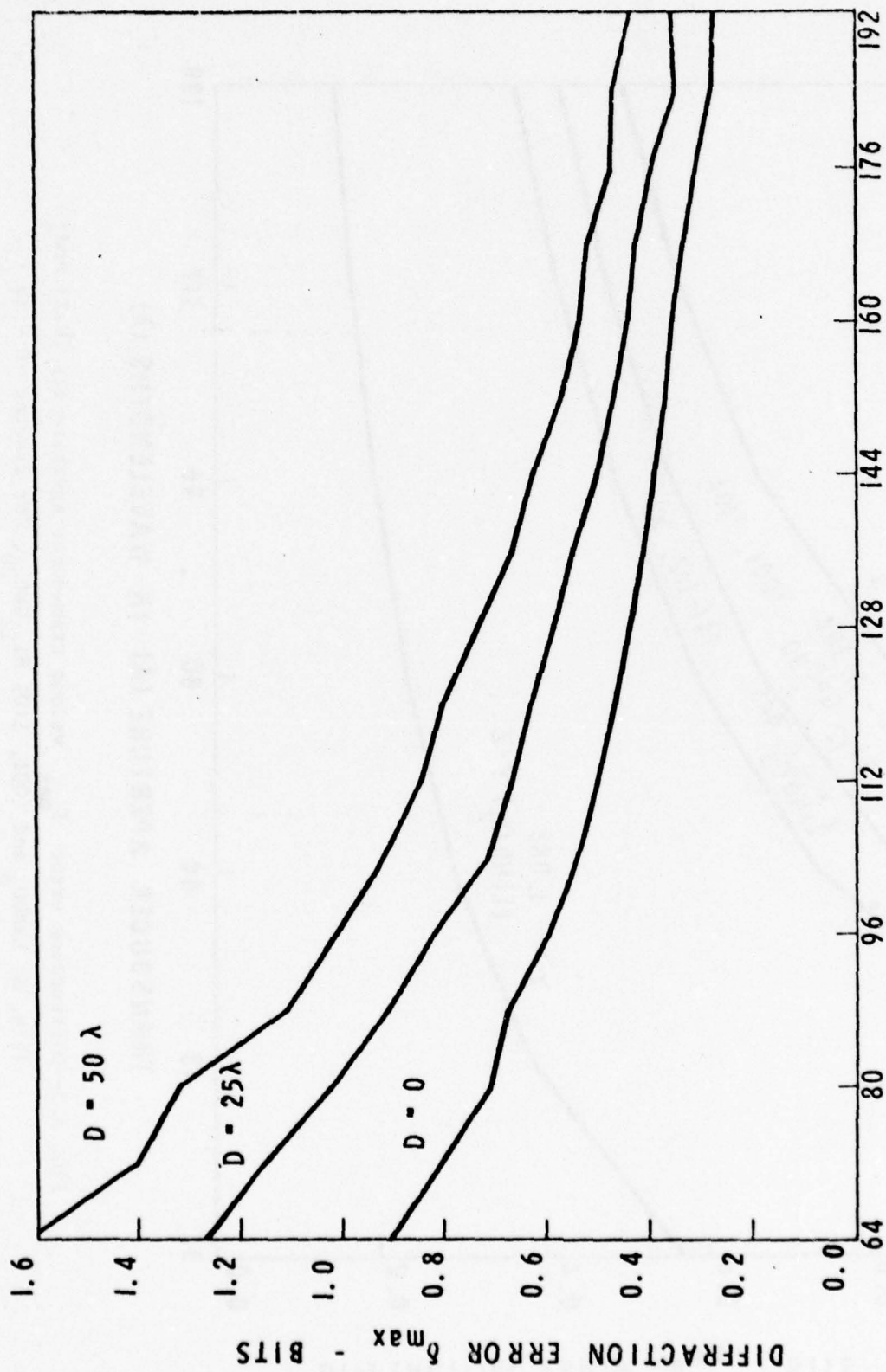FIG. A.1--Distorted output signal due to diffraction.

FIG. A.2--Diffraction error δ_{max} versus transducer aperture for various transducer spacings for ST-quartz ($\gamma = 0.378$).
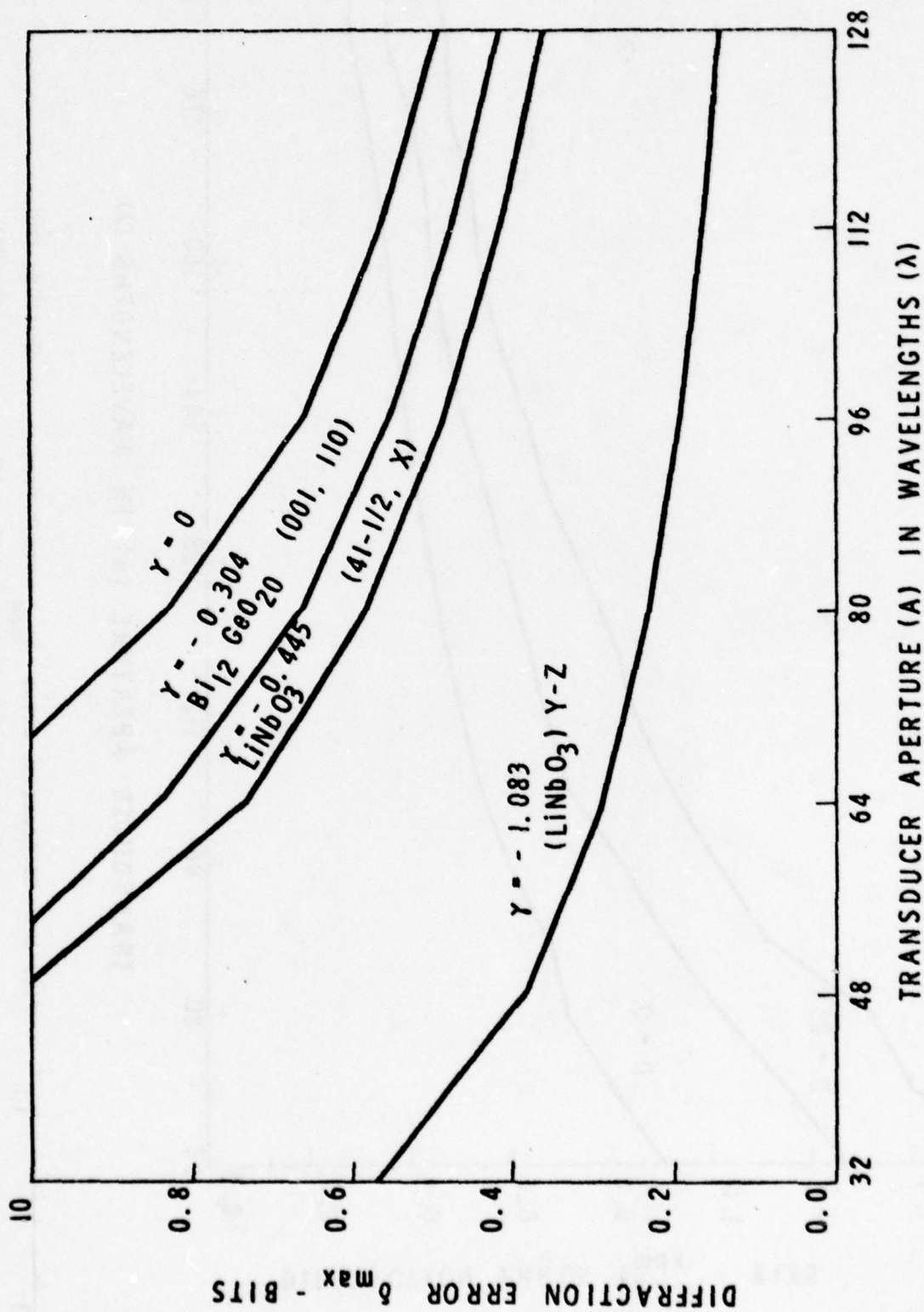
TRANSDUCER APERTURE (A) IN WAVELENGTHS (λ)

DIFFRACTION ERROR δ_{max} - BITS

Y = 0

Y = - 0.304
Bi$_{12}$GeO$_{20}$ (001, 110)

LiNbO$_3$ (41-1/2, X)
Y = - 0.445

Y = - 1.083
(LiNbO$_3$) Y-Z
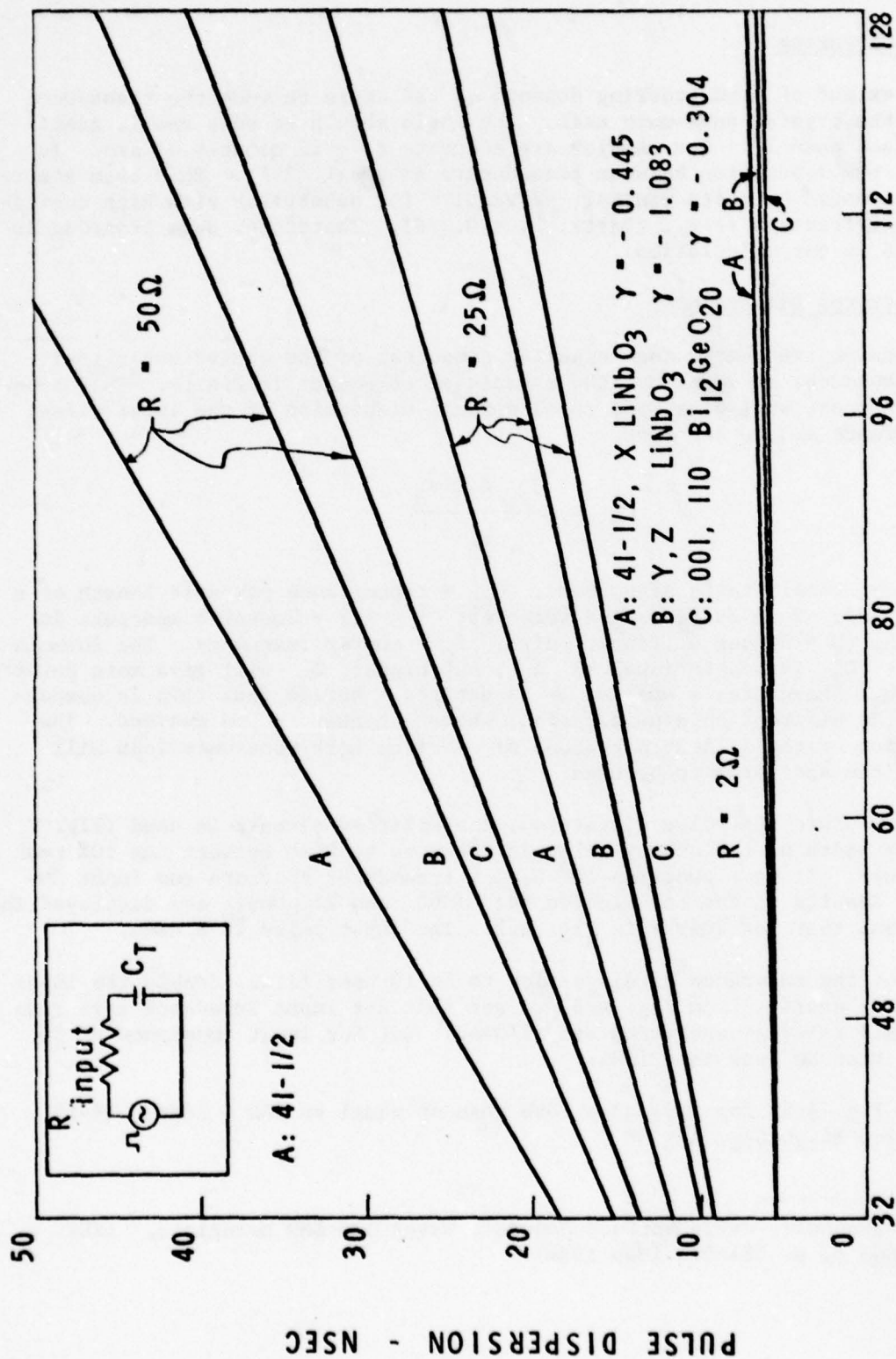
FIG. A.4--Pulse dispersion versus transducer aperture, for various values of source resistance R, for LiNbO$_3$ and Bi$_{12}$GeO$_{20}$.

TRANSDUCER APERTURE (A) IN WAVELENGTHS (λ)

PULSE DISPERSION - NSEC

R = 50Ω

R = 25Ω

R = 2Ω

A: 4I-1/2, X LiNbO$_3$ Y = - 0.445
B: Y,Z LiNbO$_3$ Y = - 1.083
C: 001, 110 Bi$_{12}$GeO$_{20}$ Y = - 0.304

A: 4I-1/2

R$_{input}$ C$_T$

4. Beam Steering

The extent of beam steering depends on the angle between the transducer axis and the crystal pure-mode axis. The angle should be very small, considerably less than 1°. Our samples are accurate to $\pm$ 15 minutes of arc. In addition, the separation between transducers is small (25λ). This beam steering effect would be quite minimal, especially for substrates with high coefficient of diffraction (e.g., quartz, $\gamma = 0.378$). Therefore, beam steering is negligible in our calculation.

5. Electrical Dispersion

At center frequency, the inductive component of the equivalent circuit of the transducer is zero, but the capacitive component is finite. This capacitive component will give rise to electrical dispersion of the input pulse. From Reference A.3 we see that

$$C_T = \frac{C_{FF} \hat{A} N V_s}{f_0}$$

where C_T = total static capacitanc, C_{FF} = capacitance per unit length of a single period, V_s = surface wave velocity, $\hat{A} = A/\lambda$ = acoustic aperture in wavelength, N = number of finger pairs, f_0 = center frequency. The formula shows that C_T is proportional to A , but higher C_T will give more pulse dispersion. Therefore, a smaller A is desired. Notice that this is competing with the diffraction consideration, where a higher A is desired. The intersection of the allowable regions of A from both considerations will determine the apertures to be used.

To calculate the pulse dispersion, a simplified circuit is used (Fig. A.4). The width of the output pulse is taken to be that between the 10% peak value points. It is a function of C_{FF} , transducer aperture and input impedance. Results of the calculation for $LiNbO_3$ and $Bi_{12}GeO_{20}$ are displayed in Fig. A.5 and that for quartz in Fig. A.2. The input pulse is 5 nsec.

We set the tolerance of dispersion to be 10 μsec (i.e., double the input value). For quartz, from Fig. A.5, we see that for input impedance less than 25 ohms, all relevant apertures are allowed. But for input impedance of 50 ohms, A must be less than 150λ.

From Fig. A.4, for impedance less than or equal to 25Ω , $LiNbO_3$ (Y-Z), $A \leq 32\lambda$; for $Bi_{12}GeO_{20}$, $A \leq 36$.

A.3 A. J. Slobodnik, Jr., "Surface Acoustic Waves and SAW Materials," IEEE Proc. 64, 5, p. 581-598 (May 1976).
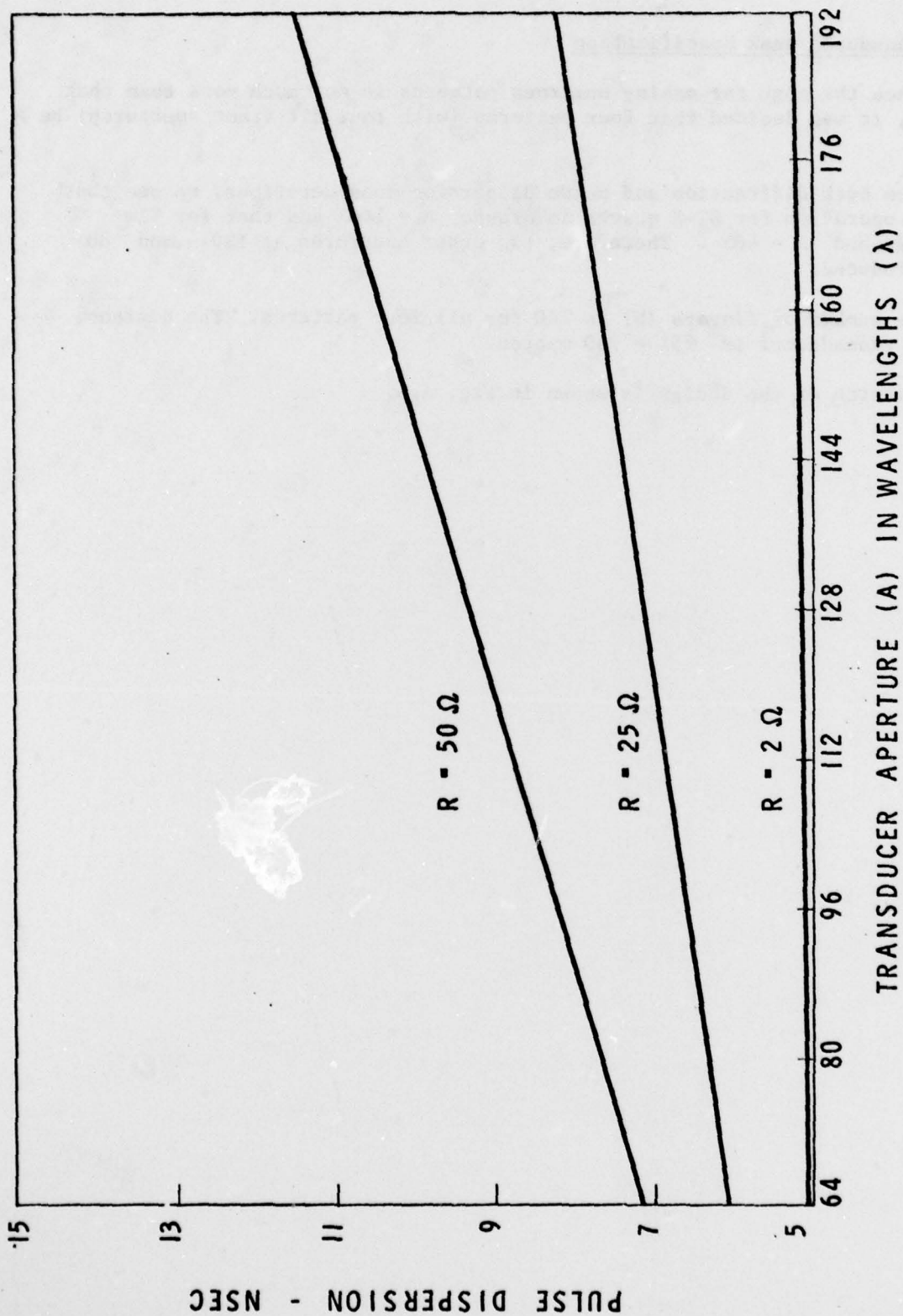
FIG. A.5--Same as Fig. A.4, for quartz.

5. Transducer Mask Specification

Since the cost for making numerous patterns is not much more than that for one, it was decided that four patterns (with four different apertures) be made.

From both diffraction and pulse dispersion considerations, we see that optimum operation for ST-X quartz is around $A = 160\lambda$ and that for YZ – LiNbO$_3$ around $A = 40\lambda$. Therefore, two other apertures at 120λ and 80λ are introduced.

The number of fingers (N) is 140 for all four patterns. The distance between transducers is $25\lambda = 780$ micron.

A sketch of the design is shown in Fig. A.6.
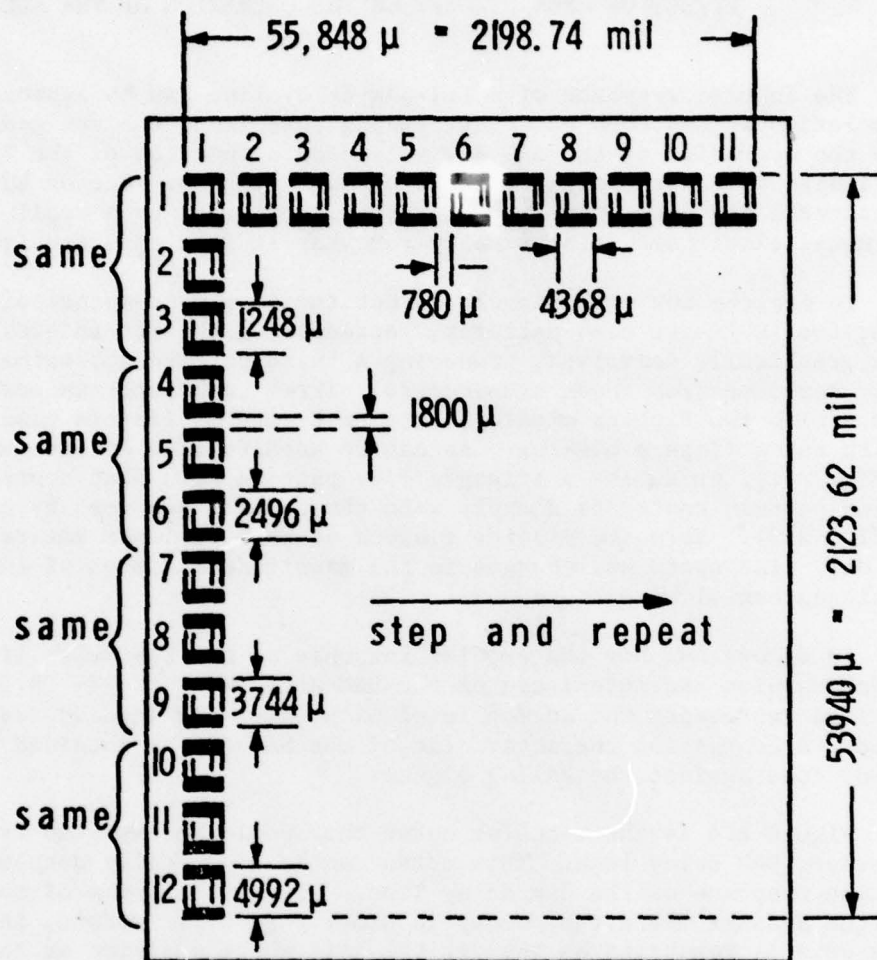
FIG. A.6--Fabrication mask for delay line transducers.

APPENDIX B

EFFECT OF OPEN FINGERS ON THE OPERATION OF THE ADC

The impulse response of a IDT-SAW delay line can be approximated by the convolution of two comb patterns. Using this fact, one can gain an insight into the operation of the SAW delay line as a function of the IDT pattern. Of particular interest are the effects of open fingers. One or both of the IDT transducers may have open fingers, usually manifest by a small break in one of the metal electrodes, electrically removing it from the circuit.

To explore how open fingers effect the impulse response of a SAW delay line, two 10 finger comb patterns, representing the interdigital transducers, were graphically convolved, producing a third pattern approximating the impulse response from those transducers. Three comb patterns were used: Pattern A with two fingers missing, Pattern B with no fingers missing and Pattern C with three fingers missing. As can be seen, Pattern A convolved with Pattern B (Fig. B.1), producing a triangle like pattern with flat spots. This convolution pattern contrasts sharply with the pattern produced by convolving A and C (Fig. B.2). Here the missing fingers of both patterns interact to produce not only flat spots but changes in the magnitude and sign of the slope in the resulting convolved pattern.

To understand how the impulse response of the SAW delay line determines the conversion characteristic of the SAW-ADC, refer to Fig. B.3. The horizontal line represents the analog level with which the impulse response is compared. A conversion characteristic of the SAW-ADC is obtained by plotting the output code against the analog signal.

Figure B.4 is the transfer curve that would be expected from the use of a perfect SAW delay line. This curve can be graphically determined from the impulse response of the SAW delay line. First, the peaks of the output are plotted against where they occur in time, Fig. B.5. Second, in Fig. B.6 the time axis is relabeled as the digital axis where position of the peaks now denotes the digital count, as the SAW-ADC method simply involves counting the number of cycles whose peak amplitude fall below the analog input. Finally, to obtain the transfer curve of the ADC from this plot, these points are simply replotted with the axes exchanged, Fig. B.7. The points are connected by straight lines to denote that the digital code remains unchanged until the amplitude of the analog signal is increased to the next higher peak or decreased to the next lower peak (in the delay line impulse response). To obtain the transfer curve for negative signals the method is simply repeated using the negative peaks of the impulse response. In Case B, one of the delay line transducers has a missing finger. The resultant impulse response shows a flat spot where the missing finger is encountered. The effect of the flat spot is seen in Fig. B.8 to produce a missing step in the ADC's transfer curve. An error of -1 LSB has been added to the $\pm \frac{1}{2}$ LSB quantizing error already present. As a rule, -1 LSB error will be added to the accuracy, or rather
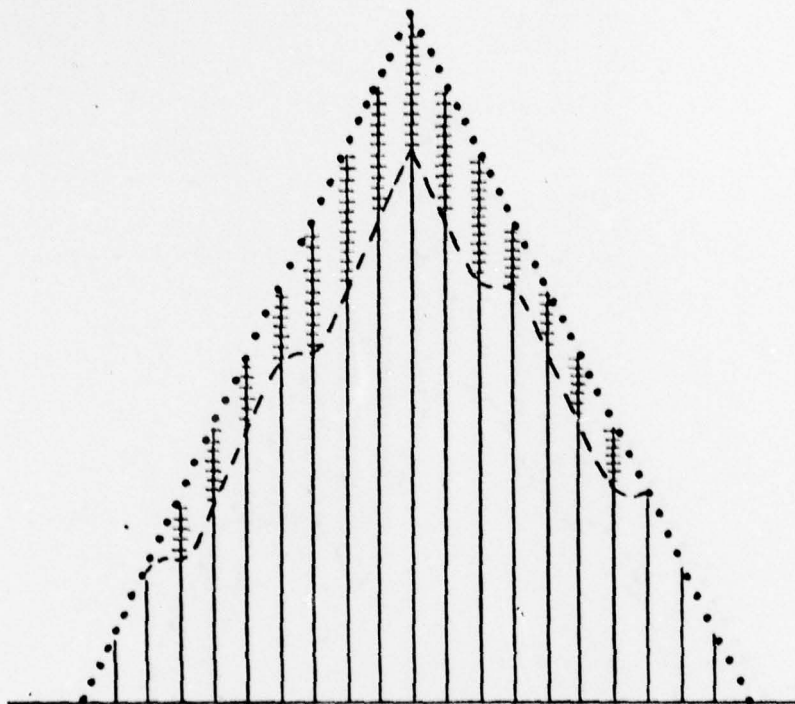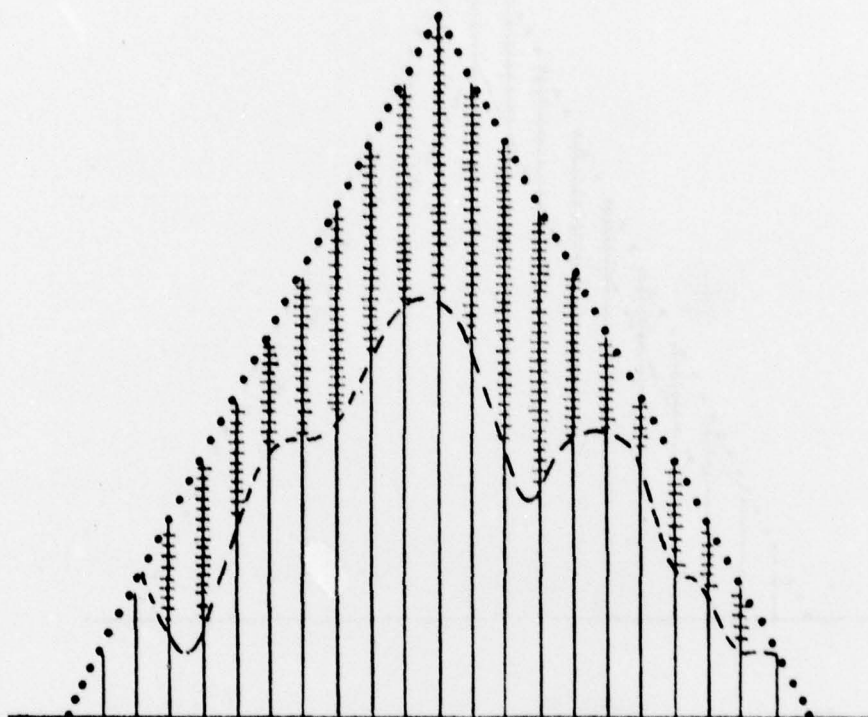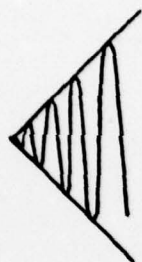
FIG. B.1--This pattern represents the convolution of two comb patterns.
One, A, represents a ten finger comb with fingers 4 and 8
missing. The other, B, represents a ten finger comb with no
fingers missing. The lines represent the magnitude of the
convolution sampled at unit intervals. The dashed line re-
presents the linear interpolation of the black lines. The
barred lines represent the magnitude of the convolution of
two ten finger combs with no fingers missing. The dotted
line represents the linear interpolation of the barred lines.
Note that the slope of the dashed line is the same as that of
the dotted except where a missing finger was incurred. The
dotted line represents the triangular shape characteristic of
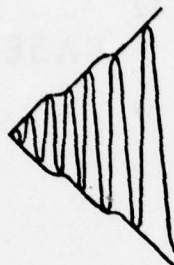the convolution of identical finite comb functions.

- 49 -

FIG. B.2--This pattern represents the convolution of two comb patterns.
One, A, represents a ten finger comb with fingers 4 and 8
missing. The other, C, represents a ten finger comb with
fingers 3, 4, and 9 missing. The lines represent the magni-
tude of the convolution sampled at unit intervals. The
dashed line represents the linear interpolation of the lines.
The barred lines represent the magnitude of the convolution
of two ten finger combs with no fingers missing. The dotted
line represents the linear interpolation of the barred lines.
Note that the first half of the dashed line is not monotonic.
Furthermore, the slope of this line differs at certain places
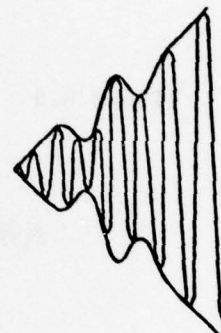from that of the dotted line.

BLAN

CASE A   CASE B   CASE C
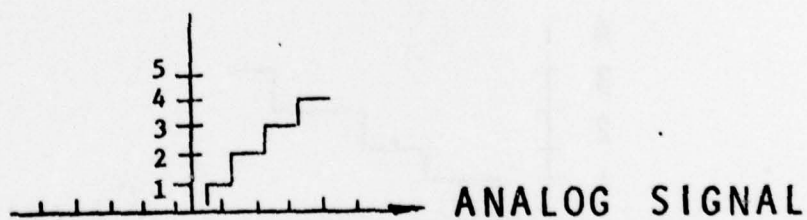
FIGURE B.3

OUTPUT CODE
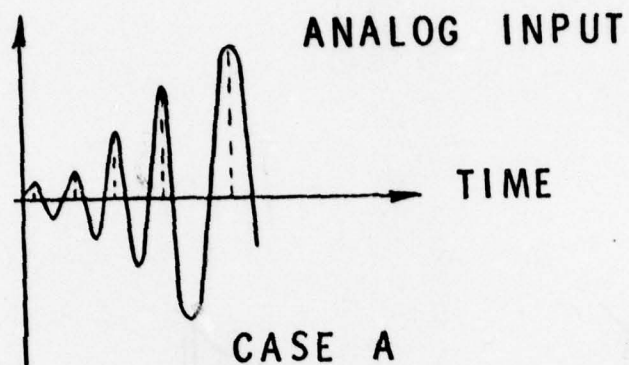
5
4
3
2
1
                              ANALOG SIGNAL

FIGURE B.4

AMPLITUDE

ANALOG INPUT

TIME

FIGURE B.5

CASE A

AMPLITUDE

DIGITAL COUNT

1 2 3 4

FIGURE B.6

OUTPUT CODE

4
3
2
1

AMPLITUDE OF
ANALOG SIGNAL
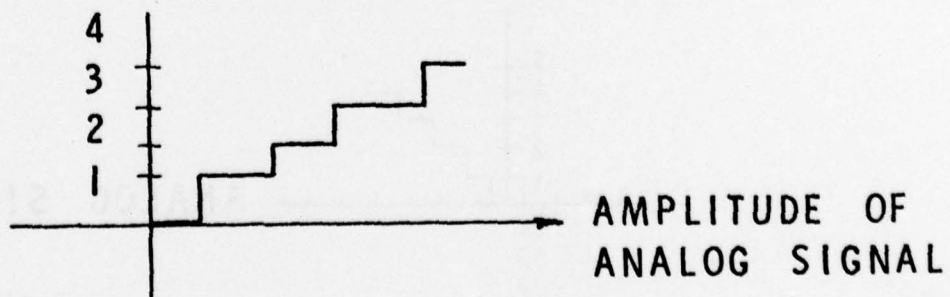
FIGURE B.7

AMPLITUDE

TIME / COUNT

1 2 3 4 5 6

OUTPUT CODE

ANALOG SIGNAL
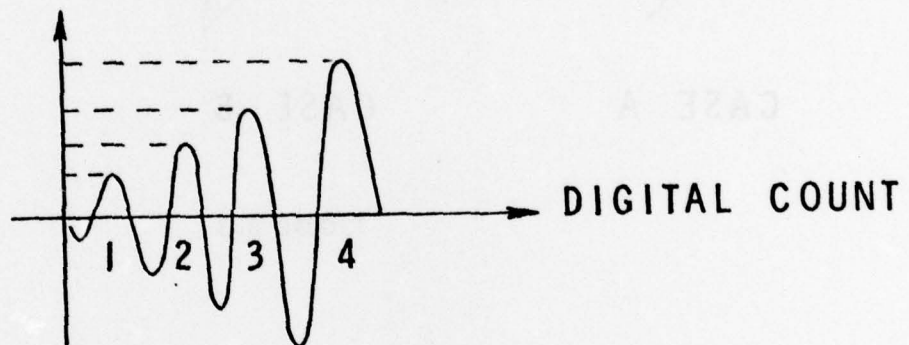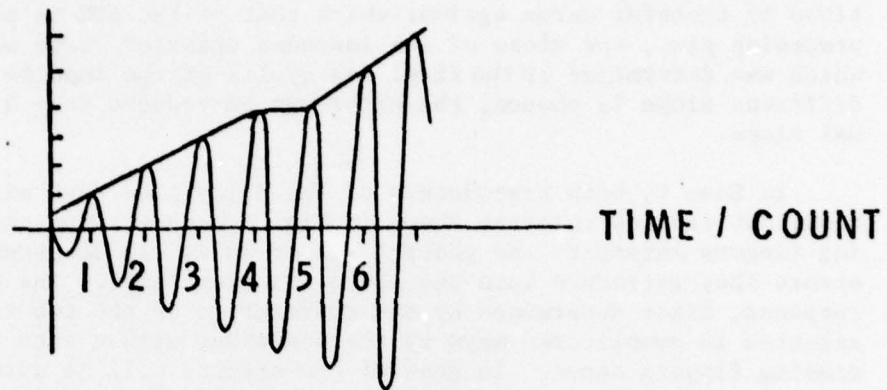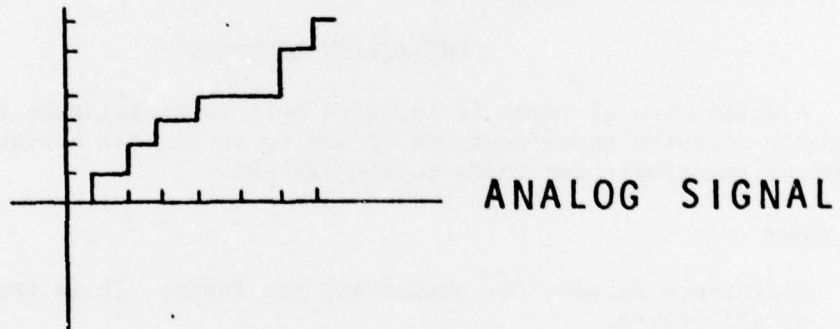
CASE B

FIGURE B.8

inaccuracy, for each missing finger in the defective transducer. This error can be reduced by choosing a different slope for the perfect straight line (of slope 1) transfer curve against which that of the ADC is compared. On the preceding plot, the slope of the intended transfer curve was chosen to be that which was determined by the first few cycles of the impulse response. If a different slope is chosen, the error can be reduced to $\pm \frac{1}{2}$ LSB times the optimal slope.

In Case C, both transducers of the delay line have missing fingers. The resultant impulse response shown in Fig. B.9 shows dips and bumps where missing fingers interact. No general set of rules can be established as to the errors they introduce into the ADC's transfer curve. The shape of the impulse response, since determined by the convolution of the two transducers, may be affected in complicated ways by the positions within each transducer where the missing fingers occur. In general the effects will be deleterious, however, since it is possible that the slope of the impulse response can increase faster than that of a perfect device, it is possible that the errors will not add in a cumulative manner. In other words, six missing fingers may not produce twice the error of three missing fingers.

An interesting feature of the SAW-A/D conversion scheme is that the transfer curve will be monotonic even though the shape of the leading edge of the impulse response of the delay line may have dips. This results from the fact that the counting of cycles stops when the <u>first</u> cycle that is greater than the analog signal is encountered. The only time a non-monotonic transfer curve was seen was when the noise level of the delay line impulse response increased to greater than $\frac{1}{2}$ LSB.

DEFINITION OF TERMS[*]

A definition of terms is included here to familiarize the reader with the commonly accepted specifications of analog to digital converters together with comments relating these terms to the SAW-ADC.

<u>Accuracy</u>

Difference between the output and the input. It is the maximum sum of all errors.
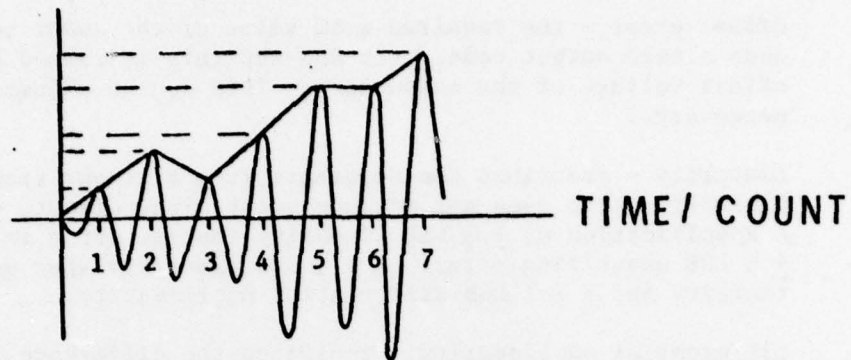
<u>Errors</u>

Quantizing error - maximum deviation from a straight line transfer function. For a perfect ADC this error would be $\pm \frac{1}{2}$ LSB.

Scale error - the departure of the actual input voltage from the design input voltage for a full scale output code. (In SAW-ADC this is caused by a change in the output of the impulser and/or a change

---

[*] Jim Sherwin, "Specifying A/D and D/A Converters," Linear Applications - Handbook 2, published by National Semiconductor.

- 54 -

AMPLITUDE

TIME/ COUNT

1 2 3 4 5 6 7

OUTPUT CODE

7
6
5
4
3
2
1

ANALOG SIGNAL
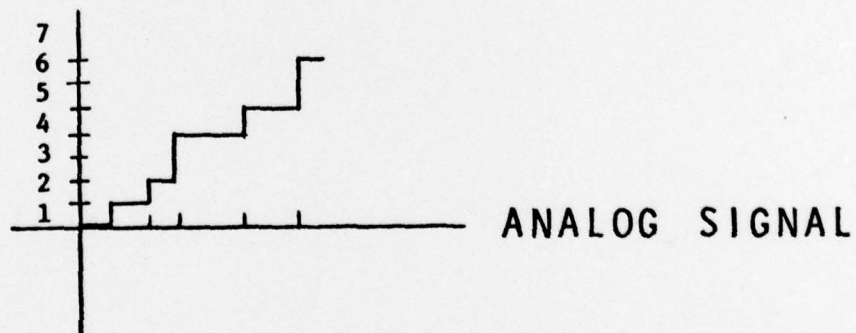
CASE C

FIGURE B.9

in the gain of the SAW amplifier - this error is removed by the division of the unknown channel by the reference channel.)

Offset error - the required mean value of the input voltage to produce a zero output code. (In SAW-ADC this is caused by the input offset voltage of the comparator. This can be adjusted to zero if necessary.)

Linearity - describes the departure from a linear transfer curve. Linearity error does not include quantizing, offset, or scale errors. A specification of $\pm \frac{1}{2}$ LSB linearity implies error in addition to the $\pm \frac{1}{2}$ LSB quantizing error. A $\pm \frac{1}{2}$ LSB linearity spec guarantees monotonieity and $\leq \pm 1$ LSB differential nonlinearity.

Differential nonlinearity - indicates the difference between the actual and the ideal voltage that produces a code change.

Monotonieity - the transfer function of a monotonic ADC will provide no decreasing output code for increasing input voltage. A $\pm \frac{1}{2}$ LSB maximum linearity spec on an n-bit converter guarantees monotonieity to n bits. A converter having greater than $\pm \frac{1}{2}$ LSB nonlinearity may be monotonic but not necessarily so.

(Linearity, differential nonlinearity, and monotonieity of the SAW-ADC is controlled by the SAW delay line. The linearity of the ADC is directly related to the linearity of the front edge of the SAW delay line impulse response. Scale, offset, and hysteresis errors are a function of the electronics and can be minimized by design and/or adjustment.)